

Thesis

Two-Dimensional Hubbard Model
at Low Electron Density

低電子濃度領域における2次元ハバード・モデル

Osamu Narikiyo

Institute for Solid State Physics
University of Tokyo

December 1991

1

Thesis

Two-Dimensional Hubbard Model
at Low Electron Density

Osamu Narikiyo

Institute for Solid State Physics
University of Tokyo

December 1991

ACKNOWLEDGEMENTS

I would like to express my sincere thanks to Prof. Hidetoshi Fukuyama for his kind supervision, stimulating discussions and encouragement since the very start of my study in the condensed matter theory.

I am very grateful to Prof. Yasumasa Hasegawa who is the kind adviser and the coworker of the study in this Thesis where many results are owing to him.

I am also grateful to my superior researchers at ISSP who illuminated me, especially to Drs. Hiroshi Matsukawa, Masao Ogata, Kazuhiro Kuboki and Hiroshi Kohno.

I also thank my colleagues of Fukuyama school for fruitful discussions.

I express my gratitude to Mrs. Shizue Maruyama for her continuous hearty encouragement.

CONTENTS

1. Introduction	1
2. Fermi Liquid and Luttinger Liquid	4
3. Anderson's Argument	10
4. Perturbative Analysis	16
4.1. Model	16
4.2. Particle-Particle Correlation Function	17
4.3. Particle-Hole Correlation Function	20
4.4. Second Order Perturbation in U	21
4.5. Third Order Perturbation in U	24
5. t -matrix Approximation	26
5.1. Poles and Analyticity of t -matrix	26
5.2. Phase Angle	28
5.3. Electron Self-energy	30
5.4. Imaginary Part of Self-energy	31
5.5. Real Part of Self-energy	33
5.6. Landau Interaction Function	35
5.7. Upper Hubbard Band and Luttinger Fermi Surface	36
5.8. Cut-off Momentum	39
5.9. Shift in Chemical Potential	40
5.10. Anisotropy in Band	41
6. Self-consistent t -matrix Approximation	44
7. Case of Attractive Interaction	48
8. Summary and Discussions	51

Appendixes	57
A. Particle-Particle Correlation Function in 2D	57
B. Particle-Hole Correlation Function in 2D	58
C. Equivalence of $\delta_{SC}(Q, \omega)$ and $\delta(Q, \omega)$	59
D. Thermodynamic Potential in t -matrix Approximation	61
E. Hubbard Approximation	62
F. Beyond t -matrix Approximation	64
F.1. Particle-Hole Channel	64
F.2. Particle-Particle Channel	64
F.3. Landau Theory vs Kohn-Luttinger Mechanism	65

References	67
------------	----

Figure Captions	70
-----------------	----

Figures	
---------	--

1. Introduction

The discovery of high- T_c oxide superconductors¹ has been attracting great interest in the study of correlations among two-dimensional electrons.^{2,3,4,5} The two-dimensional Hubbard model is the simplest one for theoretical studies. We will consider it in this Thesis expecting that it already contains the essence of the strong correlation of electrons. In spite of its simplicity, we know little about the nature of the electrons described by the Hubbard model except for the half-filled case where the system is an antiferromagnetic insulator. In this case charge fluctuations are completely suppressed at low-energy excitations and the system is effectively described only by spin degrees of freedom (the Heisenberg hamiltonian); spin and charge degrees of freedom are separated completely. In other words the system is renormalized into the strong-coupling limit for non-zero values of interaction where the charge density is frozen but the spin can move by exchange processes without changing the charge density. In contrast it is very difficult to discuss the cases for general fillings. For other dimensions we can say something conclusive in the limit of low-electron density; the system is the Luttinger liquid⁶ corresponding to the strong-coupling limit in 1D and the Fermi liquid⁷ corresponding to the weak-coupling limit in 3D. In 2D the existence of a subtlety even in the limit of low electron density was pointed out by Anderson^{8,9,10,11,12} and he concluded that the system was the Luttinger liquid. In the Fermi-liquid ground state the momentum distribution function, $n(k)$, has a jump at $k = k_F$; $n(k_F - 0) - n(k_F + 0) = Z_{k_F}$ ($0 < Z_{k_F} < 1$). Here Z_{k_F} is the quasi-particle weight at the Fermi energy. In the Luttinger-liquid ground state Z_{k_F} vanishes where an elementary excitation is not described by an electron but a spinon (collective spin excitation) and a holon (collec-

tive charge excitation). There occurs the spin-charge separation. Such a possibility in 2D deserves a serious consideration.

The central issue of this Thesis is to study whether the ground state of the two-dimensional electron system described by the Hubbard model in the limit of low-electron density is the Luttinger liquid or the Fermi liquid. We investigate it based on the t -matrix approximation, which is to be justified, within the conventional many-body theory. The strategy is as follows. First we obtain the analytic expression for the t -matrix. Then we establish the analyticity of the t -matrix and thus that of the electron self-energy. With the help of this analyticity we determine the energy dependence of the real part of the self-energy through the direct calculation of the imaginary part of the self-energy by the Kramers-Kronig relation. The real part determines the quasi-particle weight at the Fermi energy which serves as a criterion to distinguish the Fermi liquid from the Luttinger liquid.

The organization of this Thesis is as follows.

We will review the Fermi- and Luttinger-liquid concepts briefly in the next chapter and the Anderson's scenario in the following chapter. In Chap.4 we will carry out a perturbative analysis in terms of the interaction first and then show that the t -matrix approximation, the particle-particle ladder approximation up to infinite order in the interaction, can be formulated as the low-density expansion even in 2D. Then we will study the analytic properties of the t -matrix in detail and determine the quasi-particle weight at the Fermi energy in this approximation in Chap.5. Higher order contributions in the low-density expansion based on the t -matrix approximation will be examined in Chap.6. In Chap.7 we will extend the t -matrix approximation to the case of an attractive interaction. A summary will be given in the final chapter.

2. Fermi Liquid and Luttinger Liquid

In this chapter we briefly review the concepts of the Fermi liquid corresponding to the weak-coupling limit and the Luttinger liquid corresponding to the strong-coupling limit.

The Fermi-liquid state has a finite overlap with the non-interacting state. In the non-interacting state the single-particle Green's function is given by

$$\begin{aligned} G_0(k, \varepsilon) &= 1/[\varepsilon + \mu_0 - \varepsilon_k + i \cdot \text{sgn}(\varepsilon_k - \mu_0)] \\ &= 1/[\varepsilon - \xi_k + i \cdot \text{sgn}(\xi_k)], \end{aligned} \quad (1)$$

where ε_k is the band energy, the energy, ε , is measured from the chemical potential, $\mu_0 = \varepsilon_{k_F}$, which defines the Fermi momentum, k_F , and $\xi_k \equiv \varepsilon_k - \varepsilon_{k_F}$. For interacting electrons the Green's function is modified by the self-energy, $\bar{\Sigma}(k, \varepsilon)$, ($\text{sgn}[\text{Im}\bar{\Sigma}(k, \varepsilon)] = -\text{sgn}(\varepsilon)$) and given by

$$\begin{aligned} G(k, \varepsilon) &= 1/[\varepsilon + \mu - \varepsilon_k - \bar{\Sigma}(k, \varepsilon)] \\ &= 1/[\varepsilon - \xi_k - \Sigma(k, \varepsilon)], \end{aligned} \quad (2)$$

where ε is measured from the renormalized chemical potential, $\mu = \mu_0 + \bar{\Sigma}(k_F, \varepsilon = 0)$, and $\Sigma(k, \varepsilon) \equiv \bar{\Sigma}(k, \varepsilon) - \bar{\Sigma}(k_F, \varepsilon = 0)$. It should be noted that $\text{Im}\bar{\Sigma}(k, \varepsilon) = \text{Im}\Sigma(k, \varepsilon)$ because $\bar{\Sigma}(k_F, \varepsilon = 0)$ is a real energy shift. The Fermi surface is defined by

$$\mu_0 - \varepsilon_k = 0 \quad (3)$$

for non-interacting electrons and

$$\mu - \varepsilon_k - \bar{\Sigma}(k, \varepsilon = 0) = 0 \quad (4)$$

for interacting electrons. The Luttinger sum rule says that the total number of electrons, which is invariant under the introduction of an interaction, is given by a number of momentum states enclosed by the

Fermi surface. For the case with spherical symmetry the Fermi momentum for non-interacting electrons, k_F , also defines the one for interacting electrons; the volume enclosed by the spherical Fermi surface is invariant under the introduction of the interaction so that k_F is invariant. In this case the shift in the chemical potential is cancelled by the contribution from anomalous diagrams¹³ where the same state appears as both a particle and a hole. In the absence of the spherical symmetry, for example, in the case of electrons with *s*-wave interaction in an anisotropic band, the Fermi momentum depends on the direction in the momentum space, $\hat{\Omega}$, and the Fermi surface deforms by the introduction of the interaction;

$$k'_F(\hat{\Omega}) \neq k_F(\hat{\Omega}) \quad (5)$$

where $k'_F(\hat{\Omega})$ and $k_F(\hat{\Omega})$ are the Fermi momentum with and without interaction, respectively. In this case the cancellation between the shift in the chemical potential and the contribution from anomalous diagrams are broken in general. Even in this case the volume enclosed by the Fermi surface is conserved under the introduction of the interaction.

The full Green's function for low energies near the Fermi surface is divided into two parts, the contributions from the singular function of the quasi-particle pole, $G_{QP}(k, \varepsilon)$, and the non-singular function of the incoherent part, $G_{inc}(k, \varepsilon)$;

$$G(k, \varepsilon) = G_{QP}(k, \varepsilon) + G_{inc}(k, \varepsilon) \quad (6)$$

where

$$G_{QP}(k, \varepsilon) = \frac{Z_k}{\varepsilon - \xi_k^* + i \cdot \text{sgn}(\xi_k^*)} \quad (7)$$

and

$$Z_k = [1 - \frac{\partial}{\partial \varepsilon} \text{Re}\Sigma(k, \varepsilon \rightarrow 0)]^{-1} \quad (8)$$

with $\xi_k^* = v_F^*(k - k_F)$ and $v_F^* = Z_{k_F} [\partial \epsilon_k / \partial k (k \rightarrow k_F) + \partial \Sigma / \partial k (k \rightarrow k_F, \epsilon \rightarrow 0)]$. Here Z_k is the quasi-particle weight and the measure of the overlap between the interacting and the non-interacting states. Z_k appears in the momentum distribution function given by

$$n(k) = \int_{-\infty+i0}^{\infty+i0} \frac{d\varepsilon}{2\pi i} G(k, \varepsilon). \quad (9)$$

For non-interacting electrons

$$n(k) = \theta[k_F - k] \quad (10)$$

as shown in Fig.1. For interacting electrons

$$n(k < k_F) = Z_k + \int_{-\infty+i0}^{\infty+i0} \frac{d\varepsilon}{2\pi i} G_{inc}(k, \varepsilon) \quad (11)$$

and

$$n(k > k_F) = \int_{-\infty+i0}^{\infty+i0} \frac{d\varepsilon}{2\pi i} G_{inc}(k, \varepsilon). \quad (12)$$

Thus

$$n(k_F - 0) - n(k_F + 0) = Z_{k_F}. \quad (13)$$

In the Fermi-liquid state Z_{k_F} is finite ($0 < Z_{k_F} < 1$) where $n(k)$ has a jump at $k = k_F$ of Z_{k_F} as depicted in Fig.2. The non-interacting electrons corresponds to $Z_{k_F} = 1$. In the Luttinger-liquid state (ever realized only in 1D) Z_{k_F} vanishes ($Z_{k_F} = 0$) where $n(k)$ is continuous at $k = k_F$ as depicted in Fig.3. $Z_{k_F} = 0$ means that an electron is no longer a good excitation of the Luttinger liquid once an interaction is introduced. In known 1D case an elementary excitation is a spinon (collective spin excitation) and a holon (collective charge excitation). By taking these excitations as a basis, the zeroth-order fixed-point hamiltonian for 1D Hubbard model is given by

$$H_{1D}^* = \sum_q [v_s q b_{sq}^\dagger b_{sq} + v_c q b_{cq}^\dagger b_{cq}] \quad (14)$$

where b_{sq}^\dagger and b_{cq}^\dagger are the bosonized representations of the collective spin and charge excitations with velocities v_s and v_c , respectively. Here occurs the spin-charge separation. Not only in the Fermi-liquid state but also in the Luttinger-liquid state the Luttinger sum rule holds. Reflecting this fact the derivative of $n(k)$ diverges at $k = k_F$ in the Luttinger liquid state.

The long-distance and long-time physics in the Luttinger-liquid state is governed by spinons and holons which have gapless linear dispersions.^{14,15} The behavior of the thermodynamic quantities in the Luttinger-liquid state can not be distinguished from that in the Fermi-liquid state; the compressibility, κ , the susceptibility, χ , and the specific heat, γ , are given as follows

$$\kappa \propto \frac{1}{v_c}, \quad \chi \propto \frac{1}{v_s}, \quad \gamma \propto \frac{1}{v_c} + \frac{1}{v_s}. \quad (15)$$

The difference is seen in the correlation functions; for example, the electron Green's function, $G(r, t) = \langle c_s^\dagger(r, t) c_s(0, 0) \rangle$, the charge density correlation function, $N(r, t) = \langle n(r, t) n(0, 0) \rangle$, with $n(r, t) = n_1(r, t) + n_l(r, t)$, and the spin density correlation function, $S(r, t) = \langle S_z(r, t) S_z(0, 0) \rangle$, with $S_z(r, t) = \frac{1}{2}[n_1(r, t) - n_l(r, t)]$. Both spinons and holons lead to the anomalous power-law behavior of the correlation functions as follows

$$G(r, 0) \sim r^{-\eta} \cos(k_F r) \quad (16)$$

with

$$\eta = \frac{(\alpha_c + 4)^2}{16\alpha_c}; \quad \alpha_c = 2Z_c(D)^2, \quad (17)$$

$$N(r, 0) \sim \text{const.} + A_0 r^{-2} + A_2 r^{-\alpha_s} \cos(2k_F r) + A_4 r^{-\alpha_c} \cos(4k_F r) \quad (18)$$

with

$$\alpha_s = 1 + \frac{\alpha_c}{4}, \quad (19)$$

and

$$S(r, 0) \sim \text{const.} + A_0' r^{-2} + A_2' r^{-\alpha_c} \cos(2k_F r) \quad (20)$$

where $Z_c(D)$ is given by

$$Z_c(k) - \int_{-D}^D dk' \cos k' R(\sin k - \sin k') Z_c(k') = 1 \quad (21)$$

with

$$R(x) = \int_{-\infty}^{\infty} \frac{d\omega}{2\pi} \exp(-i\omega x) [1 + \exp(|\omega|)]^{-1} \quad (22)$$

and D being the holon Fermi level fixed by the electron density. Here the $4k_F$ -oscillation comes from the contribution of holons and the $2k_F$ -oscillation involves both spinons and holons. Related to the anomalous power-law behavior of the electron Green's function, $G(r, 0)$, where an electron is a composite of a spinon and a holon, the momentum distribution function is given by

$$n(k) = n(k_F) - \text{const.} \cdot |k - k_F|^\theta \cdot \text{sgn}(k - k_F) \quad (23)$$

with

$$\theta = \eta - 1 = \frac{(\alpha_c - 4)^2}{16\alpha_c}. \quad (24)$$

The scaling relations as Eq. (19), Eq. (24) and

$$\alpha_c = \frac{4\hat{\kappa}}{2\hat{\gamma} - \hat{\chi}}, \quad (25)$$

where $\hat{\kappa}$, $\hat{\gamma}$ and $\hat{\chi}$ are normalized to be unity for the non-interacting state, hold universally in the Luttinger-liquid state.

The Landau interaction function, $f_{kk'}$, which represents the change in the energy of the quasi-particle k by injecting a quasi-particle k' into the system, is given microscopically by

$$f_{kk'} = Z_k Z_{k'} \Gamma_{kk'}^\omega \quad (26)$$

where $\Gamma_{kk'}^\omega = \lim_{\omega \rightarrow 0} [\lim_{q \rightarrow 0} \Gamma_{kk', ee'}(q, \omega)]$ and $\Gamma_{kk', ee'}(q, \omega)$ is the interaction vertex defined in Fig.4. While it is finite in the Fermi-liquid state, $f_{kk'}$ is marginally finite on the Fermi surface in the Luttinger-liquid state where $\Gamma_{kk'}^\omega$ diverges so that Z_k vanishes. In terms of $f_{kk'}$ the quasi-particle energy is given by

$$\tilde{\xi}_k = \xi_k^* + \frac{1}{N} \sum_{k'} f_{kk'} \delta n_{k'} \quad (27)$$

where $\delta n_{k'}$ is 1 for a particle state and -1 for a hole state.

In 1D Luttinger-liquid state $Z_{k_F} = 0$ is the consequence of the unrenormalizable phase shift on the Fermi surface due to the fact that the injection of a particle in the system deforms the entire Hilbert space. Thus the overlap between the interacting and the non-interacting states vanishes. This is also ascribed to the fact that a particle moving in the system from one boundary to the other necessarily meets all the other particles. It results in the finite phase shift even at the Fermi energy representing the absence of a freely moving quasi-particle. An electron motion causes so strong backflow, which can be represented by a gauge field, that the electron is screened out. This phase shift or gauge field modifies the statistics of the original particle. It is realized as a change in the boundary condition in 1D; for example, the two electron ground state of the Hubbard model with infinite strength of the interaction for opposite spins is that of the hard-core boson where the corresponding boundary condition gives an extra phase shift and changes the statistics; the statistical transmutation.^{16,17}

3. Anderson's Argument ^{8,9,10,11,12}

Anderson presented two types of scenario leading to the spin-charge separated non-Fermi liquid state.

(I) large Coulomb interaction

In the effective low-energy theory in the lower Hubbard band for a large Coulomb interaction projecting out the upper Hubbard band, the Hilbert space is so changed that the one-to-one correspondence between the quasi-particle state and the free particle state, which is the basic assumption of the Fermi liquid theory, will be broken. This argument is intended for general dimensions. In this context he also regards the $t - J$ model^{2,3,4,5} defined in the Hilbert space with no double occupancy of a lattice site as the model where this scenario is realized.

(II) low-dimensionality

In 2D the hard-core nature in momentum space resulting from the singular forward scattering will lead to the tomographic Luttinger-liquid state where the Luttinger-liquid concept, which holds in 1D, still holds in each radial direction in momentum space.

Anderson tried to extend the Luttinger-liquid concept to the case of higher dimensions. The essential point of his argument is the infrared catastrophe, which is realized in the Kondo and the x-ray edge problems and so on, as recognized by the orthogonality theorem

$$\langle \Psi_G(V) | \Psi_G(0) \rangle \propto \exp\left[-\frac{1}{2}\left(\frac{\delta_{SC}}{\pi}\right)^2 \ln N\right]. \quad (28)$$

Here $\langle \Psi_G(V) | \Psi_G(0) \rangle$ is the overlap integral between the N -particle ground states in the presence and absence of the potential, V , which causes the scattering phase shift, δ_{SC} . Namely $|\Psi_G(V)\rangle$ is orthogonal to $|\Psi_G(0)\rangle$ due to the fact that every momentum state suffers the phase shift because the recoil is prohibited. It should be noted that once the recoil is allowed this infrared singularity disappears.¹⁸ while the above infrared catastrophe theorem is established for potential scattering problems, Anderson applied this theorem to the interacting problem. He regarded the quasi-particle weight as an overlap integral;

$$\sqrt{Z_k} = \langle \Psi_G(N+1) | c_{k\sigma}^\dagger \Psi_G(N) \rangle \quad (29)$$

where $\Psi_G(N)$ is the N -particle ground state. For 1D Hubbard model with infinite strength of interaction, where every momentum state suffers $\pi/2$ phase shift due to the hard-core nature (incompressibility) in momentum space, the orthogonality theorem predicts

$$\langle \Psi_G(N+1) | c_{k\sigma}^\dagger \Psi_G(N) \rangle \propto \exp\left[-\frac{1}{2}\left(\frac{1}{2}\right)^2 \ln N\right] = N^{-1/8} \quad (30)$$

which leads to the vanishing quasi-particle weight in the thermodynamic limit and reproduces the known result of the exponent of the momentum distribution function. For 2D Hubbard model he defines the scattering phase shift in a finite system as

$$\frac{\delta_{SC}(Q, \omega)}{\pi} = \frac{\omega - x_0(Q)}{x_1(Q) - x_0(Q)} \quad (31)$$

where Q and ω are the total momentum and energy of two particles, respectively, $x_1(Q)$ is the energy eigenvalue for non-interacting particles next to $x_0(Q)$ which is the threshold energy for excitations and ω is the energy eigenvalue for $x_0(Q) < \omega < x_1(Q)$ in the presence of the interaction. He estimated ω in the ladder approximation at low electron density and obtained a fractional scattering phase shift on the Fermi surface

$$\delta_{SC}(Q \rightarrow 2k_F, \omega \rightarrow 0) \sim \frac{\pi}{2} \frac{1}{\ln(k_F a)} \quad (32)$$

where a is the lattice spacing. In this case the orthogonality theorem predicts

$$Z_{k_F} \propto \exp\left[-\left(\frac{\delta_{SC}}{\pi}\right)^2 \ln L^2\right] \quad (33)$$

which vanishes in the thermodynamic limit. This non-vanishing phase shift leads to the divergence in the Landau interaction function for the particles with same momentum

$$f_{kk'} = \frac{\delta_{SC}}{\pi} \frac{|\epsilon_k - \epsilon_{k'}|}{(\mathbf{k} - \mathbf{k}')^2}. \quad (34)$$

Anderson derived this result by calculating the change in the energy of the $\mathbf{k} \uparrow$ particle by the scattering from the $\mathbf{k}' \downarrow$ particle. The change was estimated by explicitly employing the scattering wave function with the finite scattering phase shift under the assumption that the recoil of particles is prohibited by the restriction in momentum space. He argues that, if we want to capture this singularity diagrammatically within the ordinary many-body theory, the contributions from anomalous diagrams¹³ are important, because the vanishing phase shift at the Fermi energy is the consequence of the cancellation between the shift in the chemical potential and the anomalous contributions. This hard-core nature in momentum space prevents an \uparrow -spin electron from occupying a \mathbf{k} -state

if the state is already occupied by a \downarrow -spin electron. This exclusion is not demanded by the Pauli principle so that he concluded that the particles obey another fractional statistics; the statistical transmutation. (It should be noted that we know from the study of anyons¹⁹ that the statistics in 2D is not represented solely by the boundary condition in contrast to 1D case because the change in the phase of the wave function by an interchange of particles, which does not necessarily involve the boundary, is path-dependent. Even in this case the gauge field description holds.) In this case the Hilbert space for interacting electrons is totally different from that for free fermions. Thus he concludes that $Z_{k_F} = 0$. Moreover he argues that the hard-core nature breaks the Luttinger sum rule which holds under the condition where the double occupancy in momentum space is allowed.

In Anderson's argument the recoil of particles is excluded so that the Friedel sum rule holds

$$\Delta n = \frac{\delta_{SC}}{\pi} \quad (35)$$

where the change in number of particles below the Fermi energy, Δn , is determined solely by the phase shift at the Fermi energy.

In the presence of such a singularity, at the level of the zeroth-order fixed-point hamiltonian, only the scattering of the particles with the same momentum is relevant and all the other scattering channels are irrelevant. Thus the fixed point hamiltonian

$$H_{2D}^* = \sum_q \sum_{\hat{\Omega}} [v_s(\hat{\Omega}) q b_{sq\hat{\Omega}}^\dagger b_{sq\hat{\Omega}} + v_c(\hat{\Omega}) q b_{cq\hat{\Omega}}^\dagger b_{cq\hat{\Omega}}] \quad (36)$$

has the same form as H_{1D}^* in which the spin-charge separation occurs in each radial direction in momentum space; the fixed-point state is the tomographic Luttinger-liquid state.

The above argument explicitly employing the scattering phase shift, δ_{SC} , is intended for 1D and 2D cases, because δ_{SC} vanishes at the Fermi energy in 3D. But Anderson regards the hard-core nature in momentum space as a manifestation of the existence of the Hubbard gap which exists regardless of the dimensionality for a large Coulomb interaction; *i.e.*, he regards the 1D and 2D cases to be always strong-coupling due to the low dimensionality. In this case the Hubbard gap prevents the continuous transformation from the non-interacting state to that with the gap. The essential concept is the projective effect in the Hilbert space. In the effective low-energy theory in the lower Hubbard band projecting out the upper Hubbard band, the Hilbert space is so changed that the one-to-one correspondence between the quasi-particle state and the free-particle state, which is the basic assumption of the Fermi-liquid theory, will be broken.

Anderson's arguments are only suggestive and not conclusive, so we have to check the following two points; (i) whether the scattering phase shift can be non-zero at the Fermi energy and if it is non-zero whether the Fermi-liquid description fails, (ii) whether the Hubbard gap exists and if it exists whether the Fermi-liquid description fails.

Let us make heuristic arguments on the dimensionality. In the renormalized theory on the Fermi surface, in 1D and 2D the scattering conserves the direction in momentum space, *i.e.*, the allowed scattering channels are restricted only in the forward and exchange scatterings, while in 3D the direction in momentum space is variable even under the restriction of the conservation of energy and momentum. On the other hand, while in 1D a particle which passes through the system from one boundary to the other has to meet all the other particles, in 2D and 3D such a particle meets only a fraction of other particles. The arguments in momentum and coordinate spaces give us mutually contradictory insights in 2D; the former leads to the Luttinger liquid and the latter to the Fermi liquid and thus the 2D case is marginal. Next, concerning the spin-charge separation, let us consider the Hilbert space without double occupancy of a lattice site. In 1D the motion of a hole never disturbs the spin configuration of the squeezed Heisenberg chain which takes only the sites, where a spin exists, into account and spins can move by exchange processes so that the spin and charge excitations are independent. It is a naive explanation of the spin-charge separation. In 2D and 3D the motion of a hole disturbs the spin configuration and thus it is expected that an elementary excitation involves both spin and charge degrees of freedom and then is electron-like.

4. Perturbative Analysis

In this chapter we study the electron self-energy of the Hubbard model by the perturbation in the interaction.

4.1. Model

The Hubbard model we study is

$$H = -t \sum_{\langle i,j \rangle, \sigma} c_{i\sigma}^\dagger c_{j\sigma} + U \sum_i n_{i\uparrow} n_{i\downarrow}, \quad (37)$$

where $c_{i\sigma}^\dagger$ and $c_{j\sigma}$ are the creation and annihilation operators of an electron with spin σ , respectively, $n_{i\sigma} = c_{i\sigma}^\dagger c_{i\sigma}$, t is a hopping matrix element between the nearest sites i and j on the square lattice, and U is the on-site interaction. We are mainly interested in the case of a repulsive interaction, $U > 0$, at absolute zero, $T=0$, and we will mention the case of an attractive interaction in Chap.7.

In this Thesis the electron density is assumed to be low, and then the energy dispersion measured from the Fermi energy is given by

$$\xi_{\mathbf{k}} = (k^2 - k_F^2)/2m, \quad (38)$$

where $m = (2t)^{-1}$ with the lattice spacing being taken as unity. For this parabolic dispersion the density of states, $N(0)$, is given by an energy-independent constant in 2D; $N(0) = m/2\pi$. In this case particle-particle and particle-hole correlation functions of non-interacting electrons, which are important theoretical ingredients in the perturbation theory, can be obtained analytically, as are given in the following sections. This dispersion has a high energy cut-off, k_c , of the order of the inverse lattice spacing.

4.2. Particle-Particle Correlation Function

The particle-particle (p-p) correlation function with momentum \mathbf{q} and energy $i\omega_l$ is defined in Fig.5 and given by

$$\begin{aligned} K(\mathbf{q}, i\omega_l) &= T \sum_{i\epsilon_n} \sum_{\mathbf{k}} G(\mathbf{k} + \frac{\mathbf{q}}{2}, i\epsilon_n) G(-\mathbf{k} + \frac{\mathbf{q}}{2}, -i\epsilon_n + i\omega_l) \\ &= \sum_{\mathbf{k}} \frac{1 - f(\xi_{\mathbf{k}+\mathbf{q}/2}) - f(\xi_{-\mathbf{k}+\mathbf{q}/2})}{\xi_{\mathbf{k}+\mathbf{q}/2} + \xi_{-\mathbf{k}+\mathbf{q}/2} - i\omega_l}, \end{aligned} \quad (39)$$

where $\epsilon_n = (2n+1)\pi T$, $\omega_l = 2l\pi T$ and $f(\xi)$ is the Fermi distribution function and

$$G(\mathbf{k}, i\epsilon_n) = \frac{1}{i\epsilon_n - \xi_{\mathbf{k}}}, \quad (40)$$

is the thermal Green's function for the non-interacting system. At absolute zero Eq. (39) with $i\omega_l \equiv z$ is written as

$$\begin{aligned} K(q, z) &= \left(\sum_{|\mathbf{k}| < k_c} - \sum_{\mathbf{k}(\xi_{\mathbf{k}+\mathbf{q}/2} < 0)} - \sum_{\mathbf{k}(\xi_{-\mathbf{k}+\mathbf{q}/2} < 0)} \right) \frac{1}{\xi_{\mathbf{k}+\mathbf{q}/2} + \xi_{-\mathbf{k}+\mathbf{q}/2} - z} \\ &= \frac{1}{(2\pi)^2} \left[\int_0^{k_c} k dk \frac{2\pi m}{k^2 + m(x_0 - z)} \right. \\ &\quad \left. - 2 \int_0^{k_F} k' dk' \int_0^{2\pi} d\phi \frac{m}{k'^2 - m(x_0 - z) + q^2/4 - k'q \cos \phi} \right], \end{aligned} \quad (41)$$

where $x_0 = 2\xi_{q/2} = (q - 2k_F)(q + 2k_F)/4m$, and ϕ is the angle between \mathbf{q} and $\mathbf{k}' \equiv \mathbf{q}/2 \pm \mathbf{k}$ and we have introduced the cut-off momentum k_c .

By noting

$$\int_0^{2\pi} \frac{d\phi}{\cos \phi - \omega} = -\frac{2\pi}{\sqrt{\omega + 1}\sqrt{\omega - 1}}, \quad (42)$$

which is valid for any complex number ω if the square root is defined to have positive real part, we can perform the integration in Eq. (41)

analytically and the result is given as²⁰

$$K(q, z) = \frac{m}{4\pi} \ln \frac{4(x_0 - z)(x_c - z)}{[-z + \sqrt{x_+ - z}\sqrt{x_- - z}]^2}, \quad (43)$$

where $x_c = \xi_{k_c+q/2} + \xi_{-k_c+q/2} = (k_c^2 - k_F^2 + q^2/4)/m$, and $x_{\pm} = \xi_{k_F} + \xi_{q \pm k_F} = q(q \pm 2k_F)/2m$. In the case $z = x + i\eta$ (x is real and η is infinitesimally small positive number), we write K as the sum of $K' + iK''$, where K' and K'' are the real and imaginary parts, respectively, is obtained as shown in Appendix A for various regions of parameters as indicated in Fig.6. In Figs.7(a,b) we show the three-dimensional plot of $K'(q, x)$ and $K''(q, x)$. Besides the logarithmic singularity at $x = 0$ for $q = 0$, $K'(q, x)$ diverges logarithmically to minus infinity at the upper bound of the continuum spectrum ($x = x_c$) (This is not seen in Figs.7(a,b) since $x_c/|x_0| \simeq (k_c/k_F)^2 = 25$ in the present numerical calculation.) and $K'(q, x)$ at the lower bound ($x = x_0$) diverges plus or minus infinity depending on whether $q > 2k_F$ or $q < 2k_F$ (equivalently $x > 0$ or $x < 0$). The x -dependences of $K'(q, x)$ and $K''(q, x)$ for several choices of q are shown in Figs.8(a ~ d).

It is instructive to give here the derivation of the imaginary part of the particle-particle correlation function to illustrate the significance of the dimensionality. The imaginary part is given by

$$K''(q, x) = \pi m \left(\sum_{\mathbf{k}(\xi_{\pm k+q/2} > 0)} - \sum_{\mathbf{k}(\xi_{\pm k+q/2} < 0)} \right) \delta[k_x^2 + k_y^2 - r^2(q, x)] \quad (44)$$

where $r^2(q, x) = m(x - x_0)$ and the integration on the circle, $k_x^2 + k_y^2 = r^2$, is masked by the Pauli principle so that we obtain

$$K'' = \frac{m}{8\pi} \Theta \quad (45)$$

where Θ is the angle for the portion of the circle which contributes to the integration and $\Theta = 0$ for $x < x_0$ and $x_c < x$, $\Theta = 2\pi \cdot \text{sgn}(x)$ for $x_0 < x < x_-$ and $x_+ < x < x_c$, and $\Theta = 4 \sin^{-1}[mx/q\sqrt{m(x-x_0)}]$ for $x_- < x < x_+$. It should be noted that the contribution from $x \sim x_0$ is singular: $\Theta = 0$ for $r^2 < 0 (x < x_0)$ and $|\Theta| = 2\pi$ for $r^2 > 0 (x > x_0)$, i.e., K'' jumps at $x = x_0$ in 2D. The jump of K'' leads to the logarithmic divergence of K' there which is related to K'' by the Kramers-Kronig relation. (In 1D K'' diverges at $x = x_0$.) This singular behavior is observed except for $q = 2k_F$ as seen from Fig. 9 because $|\Theta| = 2\pi$ is obtained however small the radius of the circle, $k_x^2 + k_y^2 = r^2$, is.

The particle-particle correlation function in d -dimension, $K_d(q, z)$, at $T = 0$ are also obtained analytically as follows

$$K_1(q, z) = \frac{m}{2\pi} \frac{1}{\sqrt{\alpha}} \left\{ \ln \frac{\sqrt{\alpha} - k_c}{\sqrt{\alpha} + k_c} - \ln \frac{\sqrt{\alpha} - (k_F + q/2)}{\sqrt{\alpha} + (k_F + q/2)} - \ln \frac{\sqrt{\alpha} - (k_F - q/2)}{\sqrt{\alpha} + (k_F - q/2)} \right\} \quad (46)$$

for 1D and

$$K_3(q, z) = \frac{m}{2\pi^2} \left\{ (k_c - k_F) + \frac{mz}{2q} \ln \frac{(k_F + q/2)^2 - \alpha}{(k_F - q/2)^2 - \alpha} + \frac{\sqrt{\alpha}}{2} \left[\ln \frac{\sqrt{\alpha} - k_c}{\sqrt{\alpha} + k_c} - \ln \frac{\sqrt{\alpha} - (k_F + q/2)}{\sqrt{\alpha} + (k_F + q/2)} - \ln \frac{\sqrt{\alpha} - (k_F - q/2)}{\sqrt{\alpha} + (k_F - q/2)} \right] \right\} \quad (47)$$

for 3D with $\alpha = (k_F + q/2)(k_F - q/2) + mz$.

4.3. Particle-Hole Correlation Function

Next we study the particle-hole (p-h) correlation function $P(\mathbf{q}, i\omega_l)$ defined in Fig.10 and given by

$$P(\mathbf{q}, i\omega_l) = T \sum_{i\epsilon_n} \sum_{\mathbf{k}} G(\mathbf{k} - \frac{\mathbf{q}}{2}, i\epsilon_n) G(\mathbf{k} + \frac{\mathbf{q}}{2}, i\epsilon_n + i\omega_l) \\ = \sum_{\mathbf{k}} \frac{f(\xi_{\mathbf{k}-\mathbf{q}/2}) - f(\xi_{\mathbf{k}+\mathbf{q}/2})}{\xi_{\mathbf{k}-\mathbf{q}/2} - \xi_{\mathbf{k}+\mathbf{q}/2} + i\omega_l}. \quad (48)$$

At $T=0$ Eq. (48) can be analytically evaluated independently of the cut-off momentum, k_c , as first derived by Stern²¹

$$P(q, z) = -\frac{m}{2\pi} \left[1 - \frac{1}{q} \{ \sqrt{\alpha_+^2 - k_F^2} + \sqrt{\alpha_-^2 - k_F^2} \} \right] \\ = -\frac{m}{2\pi} \left[1 - \frac{\sqrt{(x_+ - z)(x_- - z)} + \sqrt{(x_+ + z)(x_- + z)}}{q^2/m} \right] \quad (49)$$

where $\alpha_{\pm} = q/2 \pm mz/q$. In the case $z = x + i\eta$, $P = P' + iP''$ is obtained as shown in Appendix B for various regions of parameters as indicated in Fig.11. Here x_{\pm} is the same as in Fig.6. In Figs.12(a,b) we show the three-dimensional plot of $P'(q, x)$ and $P''(q, x)$ and they are shown in Figs.13(a~d) as a function of x for several choices of q . In contrast to $K(q, x + i\eta)$, there are no divergent singularities in $P(q, x + i\eta)$.

The particle-hole correlation function in d -dimensions, $P_d(q, z)$, at $T=0$ are also obtained analytically as follows

$$P_1(q, z) = \frac{-m}{2\pi} \frac{1}{q} \left(\ln \frac{\alpha_+ + k_F}{\alpha_+ - k_F} + \ln \frac{\alpha_- + k_F}{\alpha_- - k_F} \right) \quad (50)$$

for 1D and

$$P_3(q, z) = \frac{-m}{4\pi^2} \left[k_F - \frac{1}{2q} \{ (\alpha_+^2 - k_F^2) \ln \frac{\alpha_+ + k_F}{\alpha_+ - k_F} + (\alpha_-^2 - k_F^2) \ln \frac{\alpha_- + k_F}{\alpha_- - k_F} \} \right] \quad (51)$$

for 3D. (P_3 was first derived by Lindhard.²²)

4.4. Second Order Perturbation in U

In this and next sections we will study the perturbative contributions in second and third orders in U . Hereafter in the perturbative analysis we will omit the contribution of the diagrams as shown in Fig. 14 because they reduce to only the shift in the chemical potential and we never need the explicit value of the chemical potential.

In second order there exists only one process to the self-energy correction, which can be given either by the p-p correlation function, K , (Fig.15(a)) or the p-h correlation function, P , (Fig.15(b)). On the other hand the processes in third order consist of two new types of processes; one is given by K (Fig.16(a)) and the other by P (Fig.16(b)). We will examine these processes in detail in the following.

The electron self-energy in the second order of U , defined as $\Sigma_2(k, z)$, is expressed in terms of K and its imaginary part in the case of $z = \epsilon + i\eta$ is given as follows

$$\text{Im}\Sigma_2(k, \epsilon + i\eta) = -U^2 \sum_{\mathbf{q}} \int_0^{\epsilon} \frac{dx}{\pi} \text{Im}K(q, x + i\eta) \text{Im}G(-\mathbf{k} + \mathbf{q}, x - \epsilon - i\eta). \quad (52)$$

The integration with respect to the angle between \mathbf{k} and \mathbf{q} , ϕ' , is performed by noting that $K(q, x + i\eta)$ does not depend on the angle

$$\text{Im}\Sigma_2(k, \epsilon + i\eta) = -\frac{U^2}{2\pi^2} \int_0^{\epsilon} dx \int_0^{\infty} q dq \text{Im}K(q, x + i\eta) \text{Im}\tilde{G}(q^2, k; x - \epsilon), \quad (53)$$

where

$$\text{Im}\tilde{G}(q^2, k; x - \epsilon) = \int_0^{2\pi} \frac{d\phi'}{2\pi} \text{Im}G(-\mathbf{k} + \mathbf{q}, x - \epsilon - i\eta) \\ = -2m \text{Im}[(q^2 - q_+^2)(q^2 - q_-^2)]^{-1/2}, \quad (54)$$

with $q_{\pm} = k \pm \sqrt{k_F^2 + 2m(x - \epsilon)}$. In r.h.s. of Eq. (53) there exist singular contributions for $\epsilon \sim 0$ and $k \sim k_F$ from both $q \sim 0$ (backward scatter-

ing (b)) and $q \sim 2k_F$ (forward scattering (f)). The former process is schematically represented in Fig.17(b), where the initial state with the electron just above the Fermi surface (Fig.17(a)) is scattered with large momentum transfer together with the creation of the particle-hole pair. (Since q is the center of mass momentum, the terminology *backward* is somewhat different from the usual one, where the momentum transfer is nearly $2k_F$.) This process results in

$$\text{Im}\Sigma_{2,b}(k, \varepsilon + i\eta) \propto -\varepsilon^2 \ln \frac{1}{|k_+/k_F + O(X^2)|}, \quad (55)$$

where $k_{\pm} = k - k_F \pm m\varepsilon/k_F$, $\varepsilon_F = k_F^2/2m$ and $O(X^2) = O((\varepsilon/\varepsilon_F)^2, \varepsilon/\varepsilon_F(k/k_F - 1), (k/k_F - 1)^2)$. On the other hand the latter process depicted in Fig.17(c) yields

$$\text{Im}\Sigma_{2,f}(k, \varepsilon + i\eta) \propto -\varepsilon^2 \ln \frac{1}{|k_-/k_F + O(X^2)|}. \quad (56)$$

These can be understood as follows by noting $x \sim 0$; for $q \sim 0$ we see $\text{Im}K \propto x/q$ and $\text{Im}\bar{G} \propto \text{Re}[1/\sqrt{q^2 - q_-^2}] \sim \text{Re}[1/\sqrt{q^2 - k_+^2}]$, while for $q \sim 2k_F$ $\text{Im}K \propto \text{Re}[x/q\sqrt{q_0 - q}] \sim \text{Re}[x/q\sqrt{2k_F - q}]$ and $\text{Im}\bar{G} \propto \text{Re}[1/\sqrt{q_+ - q}] \sim \text{Re}[1/\sqrt{2k_F - q + k_-}]$ where $q_0 = 2\sqrt{k_F^2 + m\varepsilon}$. The fact that $\text{Im}\Sigma_2(k_F, \varepsilon + i\eta) \propto \varepsilon^2 \ln(|\varepsilon/\varepsilon_F|)$ has been derived previously.^{23,24,25}

It should be noted here that in 1D the breakdown of the Fermi liquid already manifests itself in second-order perturbation, which leads to $\text{Im}\Sigma_2 \propto |\varepsilon|$, *i.e.*, $\text{Re}\Sigma_2 \propto \ln|\varepsilon|$ by the Kramers-Kronig relation resulting in the vanishing Z_{k_F} , by a similar calculation as in 2D.

The same conclusion should be obtained if Σ_2 is estimated by use of P ; *i.e.*,

$$\text{Im}\Sigma_2(k, \varepsilon + i\eta) = -\frac{U^2}{2\pi^2} \int_0^{-\varepsilon} dx \int_0^{\infty} q dq \text{Im}P(q, x + i\eta) \text{Im}\bar{G}(q^2, k; x + \varepsilon). \quad (57)$$

In this way of estimation, singular contributions are extracted from regions $q \sim 0$ (Fig.17(d)) and $q \sim 2k_F$ (Fig.17(e)); when $x \sim 0$ we note $\text{Im}P \propto x/q$ and $\text{Im}\bar{G} \propto \text{Re}[1/\sqrt{q^2 - q_-^2}] \sim \text{Re}[1/\sqrt{q^2 - k_+^2}]$ for $q \sim 0$, and $\text{Im}P \propto \text{Re}[x/q\sqrt{q_0 - q}] \sim \text{Re}[x/q\sqrt{2k_F - q}]$ and $\text{Im}\bar{G} \propto \text{Re}[1/\sqrt{q_+ - q}] \sim \text{Re}[1/\sqrt{2k_F - q + k_-}]$ for $q \sim 2k_F$.

The Landau interaction function, $f_{kk'}$, which is given by Eq. (26) regarding $U^2 K(q = k + k', \omega = \varepsilon + \varepsilon')$ as $\Gamma_{kk', \varepsilon\varepsilon'}(q, \omega)$ and neglecting the renormalization, Z_k , is ill-behaving for $z = x_0$ because of the divergence of K there in 2D.

4.5. Third Order Perturbation in U

In third order of U the process given in Fig.16(a) results in

$$\text{Im}\Sigma_3^{pp}(k, \varepsilon + i\eta) = \frac{U^3}{2\pi^2} \int_0^\varepsilon dx \int_0^\infty q dq \text{Im}K^2(q, x + i\eta) \text{Im}\bar{G}(q^2, k; x - \varepsilon). \quad (58)$$

By noting that $\text{Im}K^2 = 2\text{Im}K\text{Re}K$, singular contributions due to backward and forward scattering are estimated as

$$\text{Im}\Sigma_{3,b}^{pp}(k, \varepsilon + i\eta) \propto \varepsilon^2 \left[\ln \frac{1}{|k_+/k_F + O(X^2)|} \right]^2, \quad (59)$$

$$\text{Im}\Sigma_{3,f}^{pp}(k, \varepsilon + i\eta) \propto \varepsilon^2 \ln \frac{1}{|k_-/k_F + O(X^2)|} \ln \frac{k_c}{k_F}. \quad (60)$$

The extra factor, $\ln |k_+/k_F + O(X^2)|$, from $q \sim 0$ in Eq. (59) comes from the processes as shown in Fig.17(f) and is due to the $q = 0$ nesting to lead to the logarithmic behavior of the static ($x = 0$) part of $\text{Re}K$; $\text{Re}K(q, x = 0) \propto \ln \frac{k_c}{q}$. On the other hand, for $q \sim 2k_F$ the static part of $\text{Re}K$ is a constant; $\text{Re}K(q, x = 0) = \frac{m}{2\pi} \ln \frac{k_c}{k_F}$ leading to Eq. (60).

The third order contribution given by the process of Fig.16(b) is

$$\text{Im}\Sigma_3^{ph}(k, \varepsilon + i\eta) = \frac{U^3}{2\pi^2} \int_0^{-\varepsilon} dx \int_0^\infty q dq \text{Im}P^2(q, x + i\eta) \text{Im}\bar{G}(q^2, k; x + \varepsilon). \quad (61)$$

The singular contributions Σ_{3-}^{ph} from $q \sim 0$ and Σ_{3+}^{ph} from $q \sim 2k_F$ are obtained similarly as

$$\text{Im}\Sigma_{3\mp}^{ph}(k, \varepsilon + i\eta) \propto \varepsilon^2 \ln \frac{1}{|k_\mp/k_F + O(X^2)|}. \quad (62)$$

It should be noted that in this p-h channel there is no extra logarithmic singularity, neither $\ln k_F/k_+$ nor $\ln k_c/k_F$, present in the p-p channel. This is due to the fact that because of the absence of the nesting the static part of $\text{Re}P$ is a constant both for $q \sim 0$ and $q \sim 2k_F$; $\text{Re}P(q, x = 0) = -\frac{m}{2\pi}$.

From Eqs.(59), (60) and (62) we note two important features; the first is that a special care has to be paid to the backward scattering from the p-p channel, and the second is that the forward scattering in the p-p channel dominates over the p-h channel by the factor $|\text{Re}K/\text{Re}P| = \ln \frac{k_c}{k_F}$; *i.e.*, in the low-density limit ($k_F \rightarrow 0$) the p-p channel yields the main contributions to $\text{Im}\Sigma(k, \varepsilon + i\eta)$. (The factor, $\ln \frac{k_c}{k_F}$, results from the difference between the available momentum space in the p-p channel and that in the p-h channel.)

Hence we will concentrate on the contributions from the p-p channel in the study of higher order terms in U , which are systematically treated in the t -matrix approximation; the p-p ladder approximation. This is a low-density expansion in terms of $1/\ln(k_c/k_F)$. This will be studied in the next chapter.

Based on the preceding discussions it is deduced that, except for the backward-scattering process in the p-p channel, only $\ln|\varepsilon|$ -singularity results from the higher-order processes in $\text{Im}\Sigma(k_F, \varepsilon + i\eta)$ in the present case of the 2D electron gas. These features are in contrast to the case of the 1D electrons, where there exists contributions from both p-p and p-h channels of the order $(\ln|\varepsilon|)^n$ in the $(n+1)$ -th order processes in U because of the perfect nesting.⁶ In this sense the structure of the perturbational series in 2D is distinct from that in 1D. The low-density expansion is not defined in 1D but in 2D.

5. t-matrix Approximation

We consider the t -matrix

$$T(q, z) = \frac{-U}{1 + UK(q, z)}, \quad (63)$$

where $K(q, z)$ is the p-p correlation function studied in Sec.4.2. It is established in Chap.4 that the t -matrix approximation, the p-p ladder approximation, takes account of the lowest-order contribution in $1/\ln(k_c/k_F)$ for the electron self-energy. We first examine the analytical properties of $T(q, z)$.

5.1. Poles and Analyticity of t-matrix

The poles of the t -matrix are given by

$$K(q, z) = -\frac{1}{U}. \quad (64)$$

If z moves on all Riemann planes, which correspond to different branches of square root in Eq. (43), Eq. (64) has three solutions of z for given q . Not all of these solutions are in the physical Riemann plane. By taking the exponential of both sides of Eq. (64) and taking square to remove the square root, we get the algebraic equation of the third degree of z as

$$a_0 z^3 + a_1 z^2 + a_2 z + a_3 = 0. \quad (65)$$

Here each coefficient is given by

$$a_0 = 4(\alpha - 1), \quad (66)$$

$$a_1 = -4\left[(\alpha - 3)x_0 + (\alpha - 2)\frac{k_c^2}{m} + \alpha\frac{q^2}{2m}\right], \quad (67)$$

$$a_2 = -(2x_0 + 2\frac{k_c^2}{m} - \alpha\frac{q^2}{2m})(6x_0 + 2\frac{k_c^2}{m} - \alpha\frac{q^2}{2m}), \quad (68)$$

$$a_3 = x_0(2x_0 + 2\frac{k_c^2}{m} - \alpha\frac{q^2}{2m})^2, \quad (69)$$

where

$$\alpha \equiv \exp\left(\frac{-2}{N(0)U}\right). \quad (70)$$

From Eq. (65)-Eq. (69) it is seen that there exist two poles in the physical Riemann plane in general; one on the negative real axis for $q < 2k_F$, which was found by Engelbrecht and Randeria,²⁶ and the other above the upper bound of the spectrum, which Anderson called the antibound state of particles,^{8,9} corresponding to the upper Hubbard band²⁷. There are no other physical poles on the real axis in the energy plane. Thus the t -matrix is analytic except on the real axis. This conclusion is consistent with the observation of Engelbrecht and Randeria;²⁶ the poles of the t -matrix for interacting particles in the finite system given by $K^{-1} = -U$ have one-to-one correspondence²⁸ to those for non-interacting particles given by $K^{-1} = 0$ and thus the analyticity of the t -matrix is guaranteed. We will discuss the poles and the analyticity in more detail later in Chap.7 in comparison with the case of an attractive interaction.

5.2. Phase Angle

Here we note that the phase angle for the forward scattering channel has a subtle feature. Following Anderson,¹⁰ we define the phase angle δ by

$$\tan\delta(Q, \omega) = \frac{\text{Im}T(Q, \omega + i\eta)}{\text{Re}T(Q, \omega + i\eta)} \quad (71)$$

where $Q = 2k_F + q$. In Ref.10 Anderson stressed the difference between the phase angle, δ , and the scattering phase shift, δ_{SC} . However, Engelbrecht and Randeria²⁹ have recently shown the equivalence of the two in the t -matrix approximation. (See Appendix C.) Thus Anderson's non-vanishing phase shift at the Fermi energy should be recognized in the calculation of the phase angle. In Ref. 30 Engelbrecht and Randeria denied the possibility of the non-vanishing phase angle on the Fermi surface by examining $\delta(q=0, \omega)$. However, we have found the non-vanishing phase angle even on the Fermi surface with the complete expression of $\delta(q, \omega)$ for all q and ω . This is due to the fact that the phase angle for the forward scattering, $\delta(q \rightarrow 0, \omega \rightarrow 0)$, strongly depends on the way how both q and ω approach zero. If q is fixed to 0 and $\omega \rightarrow +0$, we get $\delta \propto \sqrt{\omega}$ as has been obtained by Engelbrecht and Randeria.²⁶ However, if q and ω move on the line $\omega = x_-(Q)$ in Fig.6,

$$\tan\delta(Q, x_-(Q)) = \frac{\pi}{2(N(0)U)^{-1} + \ln(k_c/k_F)} \cdot \text{sgn}(\omega) \quad (72)$$

as $\omega \rightarrow 0$.³¹ In general $\delta(q \rightarrow 0, \omega \rightarrow 0)$ is finite for $x_0(Q) < \omega \leq x_-(Q)$. Anderson's finite scattering phase shift⁹ was obtained by examining

$$\frac{\delta_{SC}(Q, \omega)}{\pi} = \frac{\omega - x_0(Q)}{x_1(Q) - x_0(Q)} \quad (73)$$

in a finite system for a fixed Q and $x_0(Q) < \omega < x_1(Q) < x_-(Q)$ where $x_1(Q)$ is the energy eigenvalue for non-interacting particles next to $x_0(Q)$

which is the threshold energy and ω is the energy eigenvalue determined in the ladder approximation. As we will show below, this finite phase angle does not destroy the Fermi-liquid properties in the present t -matrix approximation.

In Fig.18 we show the phase angle for a fixed momentum as a function of energy. The phase angle π for $x_p < \omega < x_0$ signals the existence of the bound state. Precisely speaking, it is a two-hole antibound state.

5.3. Electron Self-energy

The self-energy of electrons in the t -matrix approximation is given by the processes shown in Fig.19,

$$\Sigma(k, i\varepsilon_n) = T \sum_{i\omega_l} \sum_{\mathbf{q}} G(\mathbf{q} - \mathbf{k}, i\omega_l - i\varepsilon_n) T(q, i\omega_l). \quad (74)$$

It is rewritten after analytic continuation as

$$\Sigma(k, \varepsilon + i\eta) = - \sum_{\mathbf{q}} \int_{-\infty}^{\infty} \frac{dx}{\pi} [n(x)G(\mathbf{q} - \mathbf{k}, x - \varepsilon - i\eta) \text{Im}T(\mathbf{q}, x + i\eta) - f(x)T(\mathbf{q}, x + \varepsilon + i\eta) \text{Im}G(\mathbf{q} - \mathbf{k}, x + i\eta)] \quad (75)$$

where $n(x)$ and $f(x)$ are the Bose and the Fermi distribution functions, respectively. Here we have used the fact that the t -matrix is analytic in the upper plane. From this expression it can be seen that the self-energy is also analytic in the upper half plane of energy. Thus the real and the imaginary parts satisfy the Kramers-Kronig relation:

$$\text{Re}\Sigma(k, \varepsilon + i\eta) = \int_{-\infty}^{\infty} \frac{dx}{\pi} \frac{P}{x - \varepsilon} \text{Im}\Sigma(k, x + i\eta). \quad (76)$$

At $T=0$ the self-energy is given by

$$\Sigma(k, \varepsilon + i\eta) = \sum_{\mathbf{q}} \int_{-\infty}^0 \frac{dx}{\pi} [G(\mathbf{q} - \mathbf{k}, x - \varepsilon - i\eta) \text{Im}T(\mathbf{q}, x + i\eta) + T(\mathbf{q}, x + \varepsilon + i\eta) \text{Im}G(\mathbf{q} - \mathbf{k}, x + i\eta)]. \quad (77)$$

It is rewritten as

$$\Sigma(k, \varepsilon + i\eta) = \sum_{\mathbf{q}} [\theta(\xi_{\mathbf{q}-\mathbf{k}}) \int_{-\infty}^0 \frac{dx}{\pi} - \theta(-\xi_{\mathbf{q}-\mathbf{k}}) \int_0^{\infty} \frac{dx}{\pi}] \times G(\mathbf{q} - \mathbf{k}, x - \varepsilon - i\eta) \text{Im}T(\mathbf{q}, x + i\eta). \quad (78)$$

The first and second terms correspond to the hole-hole and the particle-particle ladder processes, respectively.

5.4. Imaginary Part of Self-energy

At $T = 0$ the imaginary part of the self energy is given by

$$\begin{aligned} \text{Im}\Sigma(k, \varepsilon + i\eta) &= - \sum_{\mathbf{q}} \int_0^{\varepsilon} \frac{dx}{\pi} \text{Im}T(q, x + i\eta) \text{Im}G(-\mathbf{k} + \mathbf{q}, x - \varepsilon - i\eta) \\ &= - \frac{1}{2\pi^2} \int_0^{\infty} q dq \int_0^{\varepsilon} dx \text{Im}T(q, x + i\eta) \text{Im}\bar{G}(q^2, k; x - \varepsilon). \end{aligned} \quad (79)$$

The contribution from the continuum part, *i.e.*,

$$\text{Im}T(q, x + i\eta) = \frac{U^2 K''(q, x + i\eta)}{(1 + U K'(q, x + i\eta))^2 + (U K''(q, x + i\eta))^2} \quad (80)$$

with $K''(q, x + i\eta) \neq 0$, is obtained as²⁷

$$\begin{aligned} \text{Im}\Sigma(k, \varepsilon + i\eta) &\simeq - \frac{(N(0)U)^2}{4\pi} \frac{\varepsilon^2}{\varepsilon_F} \left[\frac{2 \ln(\varepsilon_F/\varepsilon_+)}{(1 + N(0)U \ln(\varepsilon_F/\varepsilon_+))^2} \right. \\ &\quad \left. + \frac{\ln(\varepsilon_F/\varepsilon_-)}{(1 + N(0)U \ln(k_c/k_F))^2} \right] \end{aligned} \quad (81)$$

$$\simeq - \frac{(N(0)U^*)^2}{4\pi} \frac{\varepsilon^2}{\varepsilon_F} \ln \frac{1}{|k_-/k_F + O(X^2)|}, \quad (82)$$

where

$$U^* = \frac{U}{1 + N(0)U \ln(k_c/k_F)} \quad (83)$$

and $\varepsilon_{\pm}/\varepsilon_F = |k_{\pm}/k_F + O(X^2)|$. Here the low-energy behavior of $\text{Im}\bar{G}$ and the numerator of $\text{Im}T$; *i.e.*, K'' are the same as discussed for the case of U^2 and the denominator of $\text{Im}T$ is estimated at $x = 0$ to be $(1 + N(0)U \ln(k_c/q))^2$. In the r.h.s. of Eq. (81) the first term from $q \sim 0$ is suppressed by the denominator and only the second term from $q \sim 2k_F$ survives.²⁷ This suppression is the Cooper effect,³² which leads to the superconductivity for an attractive interaction, due to the $q = 0$ nesting.

The pole of $T(q, x + i\eta)$ below the lower bound for $q < 2k_F$ is given by

$$x_p \simeq x_0 - \alpha \frac{x_0^2}{x_c - x_0}, \quad (84)$$

where α is defined in Eq. (70). Since $x_p < 0$, this pole contributes to $\text{Im}\Sigma$ only when $\varepsilon < 0$. The contribution from the pole, $\text{Im}\Sigma_{pole}$, can be obtained from Eq. (79) by noting

$$\begin{aligned} \text{Im}T_{pole}(q, x + i\eta) &= -U\pi\delta(1 + UK(q, x)), \\ &= -\frac{\pi\delta(x - x_p)}{\left|\frac{\partial K}{\partial x}\right|}. \end{aligned} \quad (85)$$

and

$$\left|\frac{\partial K}{\partial x}\right|_{x=x_p} \simeq \frac{mU}{4\pi} \frac{1}{|x_0 - x_p|}. \quad (86)$$

When $\varepsilon \rightarrow -0$ and $k \rightarrow k_F$, we obtain

$$\text{Im}\Sigma_{pole}(k, \varepsilon) = -\frac{\alpha}{3\sqrt{2}\varepsilon_c\varepsilon_F} \frac{|\varepsilon^3|}{\sqrt{|k_-/k_F + O(X^2)|}}, \quad (87)$$

where $\varepsilon_c = k_c^2/2m$.

If the momentum is fixed at $k = k_F$,

$$\text{Im}\Sigma_{pole}(k_F, \varepsilon) = -\frac{\alpha}{3\sqrt{2}} \frac{|\varepsilon|^{5/2}}{\varepsilon_c\sqrt{\varepsilon_F}}. \quad (88)$$

This is the result obtained by Engelbrecht and Randeria.²⁶ On the other hand if we take $\varepsilon \rightarrow 0$ and $k \rightarrow k_F$ with the condition $k_- = 0$, we obtain

$$\text{Im}\Sigma_{pole}(k, \varepsilon) \propto -\frac{\alpha\varepsilon^2}{\varepsilon_c}. \quad (89)$$

Even in the latter case the contribution from the pole is smaller by the logarithmic factor than that from the continuum, Eq. (82). Thus we conclude that the leading contribution to the imaginary part of the self-energy is of the order of $\varepsilon^2 \ln |k_-/k_F + O(X^2)|$.

5.5. Real Part of Self-energy

In the preceding sections we have shown that the t -matrix and hence the self-energy are analytic in the upper half-plane, and the imaginary part of the self-energy behaves as $\varepsilon^2 \ln |k_-|$, ($k_- \equiv k - k_F - m\varepsilon/k_F$), for small ε . From these fact it follows by use of the Kramers-Kronig relation, Eq. (76), that the real part of the self-energy should be

$$\begin{aligned} \text{Re}\Sigma(k, \varepsilon) &= c_0 + c_1\varepsilon + c_2\varepsilon^2 + \dots \\ &\quad + c'_2\varepsilon^2 \text{sgn}(k_-) + \dots, \end{aligned} \quad (90)$$

with c_0, c_1, \dots being constants. The term $\varepsilon^2 \text{sgn}(k_-)$ corresponds to the $\varepsilon^2 \ln |k_-|$ term in the imaginary part. Therefore, the renormalization factor Z_{k_F} is finite, *i.e.*, the system is the Fermi liquid. Since the effective interaction, U^* , is finite even in the limit of $U \rightarrow \infty$, Z_k is always finite.

In 2D the Fermi surface is well-defined with $Z_{k_F} \neq 0$ where the quasi-particle is also well-defined and the spin-charge separation is absent. (In 1D the Fermi surface is defined even for the Luttinger liquid with $Z_{k_F} = 0$ where the electron is not a good elementary excitation due to the spin-charge separation.)

It is instructive here to consider the energy of the system in order to ensure that the contribution of the pole leads only to the minor correction to the Fermi liquid description. The change in the ground state energy (see Appendix D), besides the positive energy shift due to the chemical potential shift, by the introduction of the interaction is given by³³

$$\Delta E = \sum_{\mathbf{q}} \int_{-\infty}^0 d\omega \frac{\delta(q, \omega)}{\pi} \quad (91)$$

so that the contribution of positive $\delta(q, \omega)$ raises the energy. For $\omega < 0$ $\delta(q, \omega)$ is always positive both for scattering and antibound states and the energy raises by the repulsive interaction. The positive phase angle, $\delta(q, \omega) = \pi$ for $x_p < \omega < x_0$, naturally explains that it is an antibound state of holes.

5.6. Landau Interaction Function

The Landau interaction function, $f_{kk'}$, which is given by Eq. (26) regarding $T(q = k + k', \omega = \varepsilon + \varepsilon')$ as $\Gamma_{kk', \varepsilon \varepsilon'}(q, \omega)$ and neglecting the renormalization, Z_k , is ill-behaving for $z = x_-$ because of the finite K'' even on the Fermi surface, while the divergence in $f_{kk'}$ for $z = x_0$ is removed. It should be noted, however, that this singularity is already present for the case of U^2 . The important fact is that the anomaly in $f_{kk'}$ itself does not directly mean the anomaly in the physical quantities in higher dimensions; for example, the quasi-particle energy is determined as Eq. (27) by the integration of $f_{kk'}$ and the measure for the anomalous $f_{kk'}$ tends to zero in the thermodynamic limit. By the same reason in our calculation of the self-energy the anomalous phase shift does not destroy the Fermi-liquid description but only leads to the logarithmic correction.

5.7. Upper Hubbard Band and Luttinger Fermi Surface

In the t -matrix approximation the upper Hubbard band emerges for large $U (\gg t)$. For $\omega \sim U$, $K(q, \omega) \simeq -(1-2n)/\omega$ and thus $T(q, \omega) \simeq -U/[1-U(1-2n)/\omega]$ where n is the density of electrons per spin. The resulting self-energy for $\varepsilon \sim U$ is given by

$$\Sigma(k, \varepsilon) \simeq \frac{Un}{1-U(1-2n)/\varepsilon}. \quad (92)$$

With this self-energy the pole of the Green's function determined by $\varepsilon - \xi_k - \Sigma(k, \varepsilon) = 0$ is located around

$$\varepsilon \simeq U(1-n) \quad (93)$$

with the spectral weight

$$Z_k \simeq \frac{n}{1-n}. \quad (94)$$

Since the lower Hubbard band spreads over the energy range, $-\varepsilon_c - 2\varepsilon_F < \varepsilon < 2\varepsilon_c + \varepsilon_F$, where $\varepsilon_F = k_F^2/2m$ and $\varepsilon_c = k_c^2/2m$, for $\varepsilon_c \ll U$ there exists a gap between the lower and the upper Hubbard bands. Even in the presence of the gap the Luttinger sum rule holds, because the shift rule for the chemical potential, $\mu = \mu_0 + \bar{\Sigma}(k_F, \varepsilon = 0)$, which guarantees the sum rule, is valid for any strength of U . The Luttinger sum rule is regarded as non-perturbative result and should be satisfied for any interacting systems including 1D cases.

Here we will compare the present result with that obtained in the Hubbard approximation³⁴ which is regarded as the particle-particle ladder approximation on a lattice site. (See Appendix E.) The resulting self-energy is given by

$$\Sigma(k, \varepsilon) = \frac{Un}{1-U(1-n)/\varepsilon}. \quad (95)$$

There is an important and interesting difference in the factor $(1-2n)$ and $(1-n)$ in the denominators of Eq. (92) and Eq. (95); in the t -matrix approximation the Pauli principle for free fermions is fully taken into account and in the Hubbard approximation the correlation between opposite spins on a lattice site is taken into account within a static approximation neglecting a motion of particles. In this case the pole of the upper Hubbard band is located around

$$\varepsilon = U \quad (96)$$

with the spectral weight

$$Z_k = n. \quad (97)$$

Note that in the Hubbard approximation the gap exists regardless of the magnitude of U . While it scales as $U(1-n)$ in the t -matrix approximation, the energy of the upper Hubbard band is independent of n in the Hubbard approximation. The spectral weight for the upper Hubbard band is so small in the present low-density regime that the violation of the Luttinger sum rule in the Hubbard approximation is invisible, but near half-filling the sum rule is broken due to the large spectral weight of the upper Hubbard band; $Z_k \simeq 1/2$. The resulting Fermi surface with broken Luttinger sum rule is a higher dimensional analogue of the holon Fermi surface in 1D concerning only charge degrees of freedom. In the Hubbard approximation the available Hilbert space is smaller than that in the t -matrix approximation, because the dynamics of particles is absent in the former and the recoil of particles is taken into account in the latter. In other words the broken Luttinger sum rule is regarded as the defect of the Hubbard approximation where the self-energy is momentum-independent, while the momentum conservation is fully taken into account in the t -matrix approximation.

We have to consider whether the existence of the upper Hubbard band in the t -matrix approximation signals the breakdown of the Fermi liquid as claimed by Anderson.^{8,9,12} The answer is already given previously because the results in the preceding sections are independent of the strength of U . In 2D the two-particle antibound state which leads to the upper Hubbard band exists for all values of U and the spectral function for each momentum state has the same analytic structure. The Hubbard splitting is irrelevant to break the quasi-particle state in both above approximations where the spectral weight is finite at the chemical potential in the lower Hubbard band. In the Hubbard approximation, however, the Luttinger sum rule is broken, though the quasi-particle state is present except for the half-filled case where the chemical potential exists in the Hubbard gap and the spectral weight there vanishes.

5.8. Cut-off Momentum

We have introduced the cut-off momentum, k_c , in the previous discussions. It is related to the original Hubbard model by the relation

$$\pi k_c^2 = 4\left(\frac{\pi}{a}\right)^2 \quad (98)$$

with a being the lattice constant. The difference in the shape of the Brillouin zone (square in the Hubbard model and spherical in the present approximation) and the dispersion (the cosine in the Hubbard model and the parabola in the present continuum approximation) is not essential for the existence of the two-hole antibound state and the two-particle antibound state. In this context the finiteness of the band width is essential. With this cut-off momentum the effective interaction, U^* , is given by Eq. (83) so that our theory surveys the weak-coupling region after all.

5.9. Shift in Chemical Potential

The determination of the chemical potential is a complicated matter. It has a great importance when we consider the ground state energy itself. But in the calculation of the Green's function we are interested in the excitation above the ground state and it is avoided because the excitation energy is measured from the chemical potential. The violation of the cancellation between the shift in the chemical potential and the contributions of the anomalous diagrams¹³ signals the difference in the Fermi surface between the perturbed and the unperturbed ground states but tells nothing about the properties of excitations above the ground state.

The shift in the chemical potential is related not only to the phase angle at the chemical potential but also to the one for every other energies. It is seen by the formula (see Appendix D) to determine the chemical potential³³

$$N_0(\mu) = N_0(\mu) + \frac{\partial}{\partial \mu} \sum_q \int_{-\infty}^{\infty} d\omega n(\omega) \frac{\delta(q, \omega)}{\pi} \quad (99)$$

where $N_0(\mu)$ is the total number of free fermions with the chemical potential μ . Here the effect of recoil is taken into account in contrast to the case of the Friedel sum rule, Eq. (35), where the recoil is excluded. Similarly Z_{k_F} is not determined solely by the phase shift at the Fermi energy as Eq. (33) due to the recoil.

5.10. Anisotropy in Band

We consider the effect of a weak anisotropy in the band. As noted in Chap.2 the anisotropic Fermi surface is deformed by the present s -wave interaction, but we neglect the contribution of anomalous diagrams. Here we examine the property of the excitation by calculating its life-time, *i.e.*, the imaginary part of the self-energy. The imaginary part in Eq. (79) is given in another way by²⁷

$$\text{Im}\Sigma(\mathbf{k}, \varepsilon + i\eta) = - \sum_{\mathbf{q}(-\varepsilon < \xi_{\mathbf{k}-\mathbf{q}} < 0)} \text{Im}T(\mathbf{q}, \varepsilon + \xi_{\mathbf{k}-\mathbf{q}} + i\eta) \quad (100)$$

for $\varepsilon > 0$. In Eq. (100) any momentum dependence of $T(\mathbf{q}, x + i\eta)$ and $G(\mathbf{k}, \varepsilon + i\eta)$ is not assumed, while Eq. (79) is obtained for the isotropic band where $T(\mathbf{q}, x + i\eta)$ is independent of the direction of \mathbf{q} . Eq. (100) is divided into three parts, I_1, I_2, I_3 ,

$$\begin{aligned} \text{Im}\Sigma(k_F(\hat{\Omega}), \varepsilon + i\eta) &= -\frac{1}{2\pi^2} \left[\int_0^{q_1} q dq \int_0^{\alpha_0} d\alpha + \int_{q_1}^{q_2} q dq \int_{\alpha_1}^{\alpha_0} d\alpha \right. \\ &\quad \left. + \int_{q_2}^{2k_F} q dq \int_0^{\alpha_0} d\alpha \right] \cdot \text{Im}T(\mathbf{q}, \varepsilon + \xi_{\mathbf{k}-\mathbf{q}} + i\eta) \quad (101) \\ &\equiv I_1 + I_2 + I_3. \end{aligned}$$

Here $q_1 = \varepsilon/v_F$, $q_2 = 2k_F - \varepsilon/v_F$, $\cos \alpha_0 = q/2k_F$ and $\cos \alpha_1 = q/2k_F + \varepsilon/v_F q$ for the isotropic band as shown in Fig. 20. It can be shown that no singular contributions result from I_1 and I_3 because the integration region of the radial direction is small; $q_1, 2k_F - q_2 \propto \varepsilon$. In this context the contribution from the pole of the t -matrix, which is a consequence of the low-dimensionality and independent of the band shape,²⁷ results in a minor correction as shown in Sec.4.4 because it is contained in I_3 for $\varepsilon < 0$. This also holds for anisotropic cases. Thus the singular contribution comes from the integration near $q \sim q_2$ in I_2 . The contribution from

$q \sim q_1$ in I_2 is suppressed by the Cooper effect, which is caused by the $q = 0$ nesting and independent of the shape of the Fermi surface, as discussed in Sec.4.4. These reasons why we pay our attention only to the contribution from $q \sim q_2$ in I_2 also hold for anisotropic bands. Next we examine the low-energy property of $\text{Im}T(\mathbf{q}, \omega + i\eta)$. For $q_1 < q < q_2$, K' is a weak function of q and ω

$$K' \sim \frac{m}{2\pi} \ln \frac{k_c}{q} \quad (102)$$

and then K'' strongly depends on q and ω

$$K'' = \frac{m}{8\pi} \Theta \simeq \frac{m}{2\pi} \frac{m\omega/q}{\sqrt{m\omega + k_F^2 - (q/2)^2}} \sim \frac{\sqrt{m}}{4\pi} \frac{\omega/v_F}{\sqrt{v_F \Delta q}} \quad (103)$$

for $\omega < v_F \Delta q$ where $\Delta q \equiv 2k_F - q$. The expression of K'' , Eq. (103), represents the masking effect due to the Pauli principle as clarified in Sec.3.2. For anisotropic bands K'' is estimated in the same manner

$$K'' \propto \Theta \propto \frac{\omega/v_F(\alpha)}{\sqrt{v_F(\alpha)\Delta q}}. \quad (104)$$

In this region K'' in the denominator of $\text{Im}T$ is negligible in comparison with K' because $\ln(k_c/q) \gg 1$. Thus we have to evaluate the following integral to discuss the singular contribution to $\text{Im}\Sigma$

$$I_2 \propto [1 + \frac{mU}{2\pi} \ln \frac{k_c}{k_F(\Omega)}]^{-2} \int_{\alpha_1}^{\alpha_0} d\alpha \int_{\varepsilon/v_F(\alpha)}^{q_c} d(\Delta q) \frac{\varepsilon/v_F(\alpha)}{\sqrt{v_F(\alpha)\Delta q}}. \quad (105)$$

For the isotropic case

$$\int_{\alpha_1}^{\alpha_0} d\alpha = \alpha_0 - \alpha_1 \propto \frac{\varepsilon/v_F}{\sqrt{v_F \Delta q}} \quad (106)$$

thus

$$I_2 \propto \varepsilon^2 \int_{\varepsilon/v_F}^{q_c} \frac{d(\Delta q)}{\Delta q} \propto \varepsilon^2 \ln |\varepsilon|. \quad (107)$$

For cases with weak anisotropy, though we should take the angular dependence of $v_F(\alpha)$ into account, such a contribution never changes the energy dependence of $\text{Im}\Sigma$.

(The effect of a weak anisotropy in the band on the imaginary part of the self-energy in U^2 is estimated by Fujimoto³⁵ and found not to modify the energy dependence $\varepsilon^2 \ln |\varepsilon|$.)

6. Self-consistent t -matrix Approximation

We have shown in Chap.4 that the t -matrix approximation is justified as the lowest-order contribution in the low-density expansion. In this chapter we consider a higher order contribution in the self-consistent t -matrix approximation. The main interest in this chapter is to clarify whether the contribution of the anomalous diagram¹³ is important to determine the property of the quasi-particle.

It should be noted that the t -matrix approximation breaks a conservation law and the Ward identity does not hold. Here we consider the self-consistent t -matrix approximation as a conserving approximation where the Ward identity holds. In this approximation we first define a generating functional, $\Phi[\tilde{G}]$, in terms of the full Green's function, \tilde{G} , as shown in Fig.21. Then the self-energy functional, $\tilde{\Sigma}[\tilde{G}]$, is determined by the following self-consistent equation

$$\tilde{\Sigma}[\tilde{G}] = \frac{\delta\Phi}{\delta\tilde{G}}, \quad (108)$$

which is diagrammatically shown in Fig.22.

In the following we will examine the self-energy perturbatively with respect to the number of the t -matrixes which automatically corresponds to the density expansion in $1/\ln(k_c/k_F)$. If we perform the expansion for one of the full Green's function in Fig.22

$$\tilde{G} = \frac{G}{1 - \tilde{\Sigma}G} \simeq \frac{G}{1 - \Sigma G} \simeq G + G\Sigma G \quad (109)$$

and retain the free part, G , for all the other Green's functions, we obtain two types of diagrams for the self-energy as shown in Fig.23 where anomalous diagrams are contained.

We will examine the imaginary part of the self-energy. The contribution of Fig.23(a) is given by

$$\begin{aligned} \text{Im}(\tilde{\Sigma} - \Sigma)(k, \varepsilon + i\eta) \\ = - \sum_{\mathbf{q}} \int_0^\varepsilon \frac{dx}{\pi} \text{Im}[G\Sigma G(-\mathbf{k} + \mathbf{q}, x - \varepsilon - i\eta)] \text{Im}T(q, x + i\eta). \end{aligned} \quad (110)$$

At low energy $G\Sigma G$ is renormalized as $G\Sigma G \simeq (Z_{k_F} - 1)G$. Thus we obtain

$$\begin{aligned} \text{Im}(\tilde{\Sigma} - \Sigma)(k, \varepsilon + i\eta) \\ \simeq -(Z_{k_F} - 1) \sum_{\mathbf{q}} \int_0^\varepsilon \frac{dx}{\pi} \text{Im}G(-\mathbf{k} + \mathbf{q}, x - \varepsilon - i\eta) \text{Im}T(q, x + i\eta). \end{aligned} \quad (111)$$

Eq.(111) is the same as Eq.(79) except the factor $(Z_{k_F} - 1)$. The contribution of Fig.23(b) is reduced to the one shown in Fig.24 by the renormalization, $G\Sigma G \simeq (Z_{k_F} - 1)G$. The contribution from the continuum of the t -matrix is given as

$$\begin{aligned} \text{Im}(\tilde{\Sigma} - \Sigma)_{\text{cont}}(k, \varepsilon + i\eta) \\ \simeq -(Z_{k_F} - 1)U^{*2} \sum_{\mathbf{q}} \int_0^\varepsilon \frac{dx}{\pi} \text{Im}K(q, x + i\eta) \text{Im}G(-\mathbf{k} + \mathbf{q}, x - \varepsilon - i\eta), \end{aligned} \quad (112)$$

by the same renormalization of the interaction as Eq.(83), $U^* = U/(1 + N(0)U \ln(k_c/k_F))$. The energy dependence is the same as that for U^2 and only the coefficient is modified. The contribution from the pole of the t -matrix is given as

$$\begin{aligned} \text{Im}(\tilde{\Sigma} - \Sigma)_{\text{pole}}(k, \varepsilon + i\eta) \\ \simeq \frac{Z_{k_F} - 1}{U} \sum_{\mathbf{q}} \int_0^\varepsilon \frac{dx}{\pi} \text{Im}T_{\text{pole}}^2(q, x + i\eta) \text{Im}G(-\mathbf{k} + \mathbf{q}, x - \varepsilon - i\eta), \end{aligned} \quad (113)$$

where we have used the fact $T_{pole}KT_{pole} = -T_{pole}^2/U$ noting that $1 + UK = 0$ at the pole. Eq.(113) is estimated by using the fact

$$T_{pole} \propto \frac{q - q_0}{q - q_p + i\eta} \quad (114)$$

and thus

$$\begin{aligned} \text{Re}T_{pole} &\propto (q - q_0) \frac{P}{q - q_p} \\ \text{Im}T_{pole} &\propto (q - q_0)\delta(q - q_p) \end{aligned} \quad (115)$$

where q_p and q_0 are given by $x = x_p(q_p)$ and $x = x_0(q_0)$, respectively. Noting that $\text{Im}T_{pole}^2 \propto \text{Re}T_{pole}\text{Im}T_{pole}$ and

$$\frac{P}{x}\delta(x) \propto \delta'(x), \quad (116)$$

we obtain

$$\begin{aligned} \text{Im}(\tilde{\Sigma} - \Sigma) &\propto \int' d\theta \int dQ(Q + \varepsilon^2)^2 \delta'(Q) \\ &\propto \int' d\theta \int dQ(Q + \varepsilon^2)\delta(Q) \\ &\propto \varepsilon^2 \int' d\theta \propto \varepsilon^{5/2}, \end{aligned} \quad (117)$$

where $Q \equiv q - q_p$, $q_p - q_0 \propto \varepsilon^2$ and $\int' d\theta \propto \varepsilon^{1/2}$ by the delta function in Eq.(113). Thus the energy dependence is unchanged from Eq.(87) and only the coefficient is modified.

From the above perturbative analysis of the density expansion the resulting energy dependence of the self-energy is the same as that for the t -matrix and only the coefficient is modified. At the same time the chemical potential is also renormalized. The shift in the chemical potential is determined order by order in $1/\ln(k_c/k_F)$ if necessary but we can avoid this task when we are interested only in excitations above the chemical potential as mentioned previously.

The existence of the Hubbard gap should be reexamined in the self-consistent t -matrix approximation. We can conclude from the perturbative analysis that there is no Hubbard splitting and the spectral weight is continuous. For example, the Green's function with n t -matrixes depicted in Fig.25 has its spectral weight in the lower Hubbard band for $-\varepsilon_F - n(\varepsilon_c + \varepsilon_F) < \varepsilon < \varepsilon_c + n(\varepsilon_c + \varepsilon_F)$ by noting that $G(k, \varepsilon)$ and $T(q, x)$ have their spectral weight for $-\varepsilon_F < \varepsilon < \varepsilon_c$ and $-2\varepsilon_F < x < 2\varepsilon_c$, respectively, where $\varepsilon_F = k_F^2/2m$ and $\varepsilon_c = k_c^2/2m$. Thus the Hubbard splitting is absent in the self-consistent t -matrix approximation where infinite number of t -matrixes are involved. The existence of the Hubbard gap in the t -matrix approximation is due to the approximation which lacks the self-consistency.

The Hubbard gap exists only for a particular circumstance; for the half-filled case. In this case the spectral weight at the chemical potential vanishes and thus the quasi-particle with gapless excitation of Fermi liquid type is absent.

7. Case of Attractive Interaction

In this section we consider the poles of the t -matrix in the case of attractive interaction ($U < 0$). There exists three characteristic regions depending on the value of U .

The first is the case of weak interaction, $0 > U > -U_{c1}$, where

$$U_{c1}^{-1} = K'(2k_F, x=0) = N(0) \ln \frac{k_c}{k_F} \quad (118)$$

as shown in Fig.8(c). In this region there is a pair of poles with finite imaginary parts of opposite signs for $q < q_c(U) = 2\sqrt{(k_c^2 - k_F^2)/(\alpha - 1)}$ which is a monotonically increasing function of $|U|$; $0 \leq q_c(U) \leq 2k_F$ for $0 \geq U \geq -U_{c1}$. (α is given in Eq. (70).) The existence of the pole in the upper half plane implies the instability of the Fermi surface against the formation of the Cooper pairs. Between q_c and $2k_F$ there are no poles in the physical plane, *i.e.*, all poles are on the other Riemann plane which can only be reached through the branch cut connecting x_+ and x_- . When $q = 2k_F$ one pole appears at $x = 0$ and this pole moves on the real axis as q increases. This pole is the two-particle bound state found by Schmitt-Rink, Varma and Ruckenstein³⁶ and the energy of this pole is determined as open circles in Fig.8(d).

If $-U_{c1} > U > -U_{c2}$, where

$$U_{c2}^{-1} = \max\{K'(q=0, x < x_0)\} = N(0) \ln \frac{k_c^2}{2k_F \sqrt{k_c^2 - k_F^2}} \quad (119)$$

as shown in Fig.8(a), there appears another critical value, q'_c , for $q < q'_c$ there is a pair of complex poles, which merges on the real axis at $q = q'_c$. For $q'_c < q < 2k_F$ two poles are on the negative real axis as seen in Fig.8(b). One of these poles moves to $x = 0$ at $q = 2k_F$ and disappears for $q > 2k_F$, while the other continues to exist for $q > 2k_F$ (Fig.8(d)).

If the attractive interaction is sufficiently strong such that $|U| > U_{c2}$, which corresponds $|U| \gg t$ in the original Hubbard model on the lattice, q'_c tends to zero; *i.e.*, for $q < 2k_F$ there are two real poles (Fig.8(a)), one of which disappears for $q > 2k_F$ (Fig.8(d)).

The q -dependences of the location of the poles for choices of $mU = -3.0, -5.0$ and -7.0 are shown in Figs.26(a ~ c). The U dependences of the poles for $q = 0$ and $q = 1.5k_F$ are shown in Figs.27(a and b). In these figures we have chosen as $k_c/k_F = 5.0$ so that $-mU_{c1} = -3.9$ and $-mU_{c2} = -6.7$.

If there is no pole for $q < 2k_F$, the instability will occur at the chemical potential; the Cooper instability, and the pole for $q > 2k_F$ will play no crucial role in the ground state.

In the case where a pair of poles appear in the negative real axis, we can identify the lower one as the bound state of particles and the other one as the antibound state of holes. The chemical potential should be shifted to the pole with lower energy below the continuum. Therefore, in this case the Fermi surface is unstable due to the bose condensation of particle pairs, which may be interpreted as the formation of real-space pairs.

So we observe the crossover between the Cooper pair for weak coupling and the real-space pair for strong coupling.

It is instructive to illustrate the analyticity of the t -matrix by the consideration of the finite system.^{26,28} The poles of the t -matrix in the finite system are given by $K^{-1} = -U$ and determined graphically as dots shown in Fig. 28. For repulsive interaction ($U > 0$) each poles below the chemical potential corresponds to the two-hole scattering/antibound state and one above the chemical potential corresponds to the two-particle scattering/antibound state, and all poles have one-to-one correspondence

to those for non-interacting holes/particles given by $K^{-1} = 0$. For attractive interaction ($U < 0$) two poles, open circles in Fig. 28, at the chemical potential are always missing in the thermodynamic limit where the bottom of K at the chemical potential tends to infinity. In the case of weak attractive interaction the missing two poles leave the real axis of energy and appear as a pair of complex-conjugate poles. In the case of sufficiently strong interaction two new poles appear; one for the two-particle bound state and the other for the two-hole antibound state.

We also found an interesting relationship between positive and negative U . As indicated in Chap.5 the t -matrix $T(q, x)$ ($0 \leq q < 2k_F$) has an isolated pole on the real axis below the lower bound of the continuum if the interaction is repulsive ($U > 0$). The existence of this pole has been noted by Engelbrecht and Randeria.²⁶ This pole is the indication that the energy to create a pair of holes is increased by the repulsive interaction of electrons. Therefore, the existence of the pole does not mean the instability of the Fermi surface. On the other hand, if the interaction is attractive and strong enough ($U < -U_{c1}$), $T(q, x)$ has two real poles. One of these poles tends to minus infinity as $U \rightarrow -\infty$, while the other one remains constant and continuously changes to the pole for the repulsive case as $1/U$ becomes -0 to $+0$. The former pole may be interpreted as the bound state of the particles in the case of attractive force, and make the Fermi surface unstable, while the latter pole will be interpreted as the antibound state of the holes in both cases of attractive and repulsive interactions.

8. Summary and Discussions

The ground state of the two-dimensional Hubbard model in the limit of low electron density is studied in the t -matrix approximation which is shown to be defined as the low-density expansion by examining the perturbative contributions with respect to the interaction.

The analytical expression of the t -matrix is obtained and there exists a singularity in the forward scattering strongly depending on both energy and momentum. The singularity results in the finite phase angle of the t -matrix even at the Fermi energy.

For repulsive interactions the quasi-particle weight at the Fermi energy is examined analytically and found to be finite in spite of the presence of the singular forward scattering so that the Fermi liquid description holds and the spin-charge separation predicted by Anderson is absent. Higher order contributions of the low-density expansion are also examined.

For attractive interactions the crossover between the Cooper pair for weak coupling and the real-space pair for strong coupling is observed in the pole of the t -matrix.

In the following we discuss our results in more detail.

First the structure of the perturbational series is investigated by the explicit evaluation of second-order and third-order contributions in U to the imaginary part of the self-energy function, $\Sigma(k, \varepsilon + i\eta)$. In second order of U we obtain $\text{Im}\Sigma(k_F, \varepsilon + i\eta) \propto \varepsilon^2 \ln|\varepsilon|$ as has been noted previously.^{23,24,25} To this singularity both forward ($q \sim 2k_F$) and backward ($q \sim 0$) scatterings in the particle-particle (p-p) channel with center-of-mass momentum, q , contribute. The same process can also be regarded as a particle-hole (p-h) channel, in which case both regions of $q \sim 2k_F$ and $q \sim 0$ of the p-h correlation function with the center-of-mass momentum of particle and hole, q , result in this singular contribution. In third order of U , there exist two distinct processes consisting of either p-p or p-h channels, where the forward scattering in the p-p channel and both $q \sim 2k_F$ and $q \sim 0$ in the p-h channel result in the same singularity $\varepsilon^2 \ln|\varepsilon|$. On the other hand the backward scattering in the p-p channel yields more singular contributions of the order $\varepsilon^2 (\ln|\varepsilon|)^2$ due to the $q = 0$ nesting. Because of this stronger singularity due to the backward scattering in the p-p channel on one hand and the fact that the contribution to $\varepsilon^2 \ln|\varepsilon|$ from the forward scattering in the p-p channel is larger than those from the p-h channel by $\ln(k_c/k_F)$, k_c being the cut-off momentum, on the other hand, the multiple scattering processes involving the p-p channel have to be taken into account in the first place. Among them the particle-particle ladder approximation corresponds to the lowest order contribution in $1/\ln(k_c/k_F)$. This is precisely the t -matrix approximation, on which our further studies are based. In this t -matrix approximation we found that the total contribution from the backward scattering suppresses the logarithmic singularity and that only the forward scattering process contributes to $\varepsilon^2 \ln|\varepsilon|$ in $\text{Im}\Sigma(k_F, \varepsilon + i\eta)$.²⁷

The suppression of the backward scattering, the Cooper effect,³² has the same origin as the superconductivity for an attractive interaction.

In order to understand the nature of electron liquid near the Fermi energy based on this knowledge of $\text{Im}\Sigma(k, \varepsilon + i\eta)$ we have to clarify the analytical property of $\Sigma(k, z)$ ($\text{Im}z > 0$) which is governed by that of the t -matrix, $T(q, z)$. By deriving the analytical expression of the p-p correlation function the location of all possible poles of the t -matrix has been clarified; the t -matrix is analytic except on the real axis in the complex energy plane, so that $\Sigma(k, \varepsilon + i\eta)$ is also analytic there. From this analyticity $\text{Re}\Sigma(k, \varepsilon + i\eta)$ is related to $\text{Im}\Sigma(k, \varepsilon + i\eta)$ by the Kramers-Kronig relation. Thus from the result of $\text{Im}\Sigma(k_F, \varepsilon + i\eta) \propto \varepsilon^2 \ln|\varepsilon|$ it is concluded that the quasi-particle weight on the Fermi surface determined by $\text{Re}\Sigma(k_F, \varepsilon + i\eta)$ is finite for any strength of U ; *i.e.*, the electrons described by the Hubbard model are Fermi liquid. So the spin-charge separation proposed by Anderson^{8,9,10,11,12} is absent in the present t -matrix approximation. The same conclusion is reached by Engelbrecht and Randeria²⁶ by a slightly different argument; $\text{Im}\Sigma(k_F, \varepsilon + i\eta) \propto \varepsilon^2 \ln|\varepsilon|$ based on the results of second order perturbation and the analyticity of the t -matrix by noting the one-to-one correspondence of two-particle scattering state in the presence and absence of interaction.

Besides the contribution of the scattering state, the bound state of the t -matrix, which is due to the low-dimensionality and found by Engelbrecht and Randeria,²⁶ contributes to $\text{Im}\Sigma(k, \varepsilon + i\eta)$. But it results in a minor correction; $\text{Im}\Sigma(k_F, \varepsilon + i\eta) \propto \theta(-\varepsilon)|\varepsilon|^{5/2}$, and thus the above conclusion is unchanged. Precisely speaking, the bound state is a two-hole antibound state and the energy is raised by the formation of the antibound state so that it has nothing to do with the instability of the Fermi surface.

On the other hand the high-energy antibound state of particles always exists regardless of the dimensionality for finite energy bands. For sufficiently large U this antibound state forms the upper Hubbard band in the t -matrix approximation and there exists the Hubbard gap. Though Anderson^{8,9,12} stressed the possible importance of the existence of the Hubbard gap concerning the analyticity of the t -matrix and self-energy, we have found no signal of the breakdown of the Fermi liquid description. At first sight the formation of the upper Hubbard band might seem to break the Luttinger sum rule as in the Hubbard approximation, it does not because the conservation of momentum holds in the t -matrix approximation while the momentum-independence of the self-energy breaks it in the Hubbard approximation. It should be noted, however, that the existence of the Hubbard gap is due to the lack of the self-consistency in the t -matrix approximation; in the self-consistent t -matrix approximation there exists no Hubbard gap however large the interaction is.

In the present study the extreme subtlety of the forward scattering has been indicated; the phase angle, $\delta(2k_F+q, \omega)$, of the t -matrix strongly depends on energy and momentum and can have a finite value at the Fermi energy if $\omega \rightarrow 0$ by keeping $\omega/v_F q = 1$. This subtlety caused an conflicting argument between Anderson¹⁰ and Engelbrecht and Randeria³⁰ but it is resolved by our result of the phase angle for all energy and momentum. Anderson^{8,9,11,12} argued that this non-vanishing phase angle destroys the Fermi liquid description due to the infrared orthogonality catastrophe, but it does not and leads only to the logarithmic correction to it by the phase space reason; the calculation of the self-energy involves this singularity but its measure vanishes in the integration.

Anderson's tomographic Luttinger liquid^{8,9,10,11,12} is not realized in 2D. The relevant interaction channel is not restricted to the singular

forward scattering. The effect of recoil, *i.e.*, the existence of the available phase space for scatterings, is significant and different from the cases of the potential scattering problems and the 1D interacting systems. Thus the analogy of the infrared catastrophe theorem is not applicable to the 2D case.

The Fermi-liquid behavior obtained in the t -matrix approximation is unchanged if we consider higher-order terms in $1/\ln(k_c/k_F)$ in the self-consistent t -matrix approximation where anomalous diagrams, whose importance Anderson^{10,12} pointed out, are taken into account.

The breakdown of the Landau's Fermi-liquid theory³⁷ might originate from the construction of the effective interaction vertex which is treated as an input parameter in the Landau theory. In this context the effect of the spin fluctuation is significant and has a possibility to lead to the superconducting ground state. In this case the effective interaction is attractive and the Cooper effect³² destroys the Fermi liquid state, while it suppresses the backward scattering for repulsive interaction. (See Appendix F.)

In the renormalization group treatment^{38,39,40} in 1D the discreteness of the Fermi surface (right and left points) has a great significance where both the Cooper channel and the zero-sound channel have the same singular contributions with opposite sign and cancel each other and this cancellation results in the marginal effective interaction which leads to the Luttinger-liquid fixed point. In 2D (circle) and 3D (sphere) the Fermi surface consists of continuous momentum states where only the Cooper channel has a singular contribution which leads to a Fermi-liquid/non-Fermi-liquid fixed point for a repulsive/attractive interaction.

In our approach the double occupation of a lattice site is always allowed so that the available Hilbert space for interacting electrons is the

same as that for free fermions. Moreover the resulting effective interaction, U^* , corresponds to the weak-coupling limit when the bare interaction, U , is finite in the low-electron density region. Therefore the concept of the projected Hilbert space corresponding to the strong-coupling limit does not seem to be involved in our perturbational treatment. If the Hilbert space is modified, the quasi-particle might be still well-defined because it is governed by the low-energy sector but the Luttinger sum rule would be broken because it concerns the entire Hilbert space. In this context a non-Fermi liquid state has been reported in the study of the $t-J$ model^{41,42} where the double occupation is excluded and the Hilbert space is totally different from that of free fermions.

The spin-charge separated Luttinger-liquid state proposed by Anderson^{8,9,11,12} is not realized in the Hubbard model but the possibility of its realization in real materials still remains.

Appendix A : Particle-Particle Correlation Function in 2D

(I) for $x < x_0$

$$K' = \frac{m}{4\pi} \ln \frac{4(x_0 - x)(x_c - x)}{[-x + \sqrt{(x_+ - x)(x_- - x)}]^2},$$

$$K'' = 0,$$

(II) for $x_0 < x < x_-$

$$K' = \frac{m}{4\pi} \ln \frac{4(x - x_0)(x_c - x)}{[-x + \sqrt{(x_+ - x)(x_- - x)}]^2}$$

$$= \frac{m}{4\pi} \ln \frac{4[x + \sqrt{(x_+ - x)(x_- - x)}]^2(x_c - x)}{(q^2/m)^2(x - x_0)},$$

$$K'' = \frac{m}{4} \operatorname{sgn}(x),$$

(III) for $x_- < x < x_+$,

$$K' = \frac{m}{4\pi} \ln \frac{4(x_c - x)}{q^2/m}$$

$$K'' = \frac{m}{2\pi} \sin^{-1} \frac{x}{\sqrt{(x - x_0)(q^2/m)}}$$

$$= \left[\frac{m}{4} - \frac{m}{2\pi} \sin^{-1} \sqrt{\frac{(x_+ - x)(x - x_-)}{(x - x_0)q^2/m}} \right] \operatorname{sgn}(x),$$

(IV) for $x_+ < x < x_c$

$$K' = \frac{m}{4\pi} \ln \frac{4(x - x_0)(x_c - x)}{[x + \sqrt{(x - x_+)(x - x_-)}]^2},$$

$$K'' = \frac{m}{4},$$

(V) for $x > x_c$

$$K' = \frac{m}{4\pi} \ln \frac{4(x - x_0)(x - x_c)}{[x + \sqrt{(x - x_+)(x - x_-)}]^2},$$

$$K'' = 0.$$

Appendix B : Particle-Hole Correlation Function in 2D

(I) for $x < -x_+$

$$P' = -\frac{m}{2\pi} \left[1 - \frac{\sqrt{(x_+ - x)(x_- - x)} - \sqrt{(x_+ + x)(x_- + x)}}{q^2/m} \right],$$

$$P'' = 0,$$

(II) for $-x_+ < x < -|x_-|$

$$P' = -\frac{m}{2\pi} \left[1 - \frac{\sqrt{(x_+ - x)(x_- - x)}}{q^2/m} \right],$$

$$P'' = \frac{m}{2\pi} \frac{\sqrt{(x_+ + x)(-x_- - x)}}{q^2/m},$$

(III) for $x_- < x < -x_-$

$$P' = -\frac{m}{2\pi},$$

$$P'' = \frac{m}{2\pi} \frac{-\sqrt{(x_+ - x)(-x_- + x)} + \sqrt{(x_+ + x)(-x_- - x)}}{q^2/m},$$

(IV) for $-x_- < x < x_-$

$$P' = -\frac{m}{2\pi} \left[1 - \frac{\sqrt{(x_+ - x)(x_- - x)} + \sqrt{(x_+ + x)(x_- + x)}}{q^2/m} \right],$$

$$P'' = 0,$$

(V) for $|x_-| < x < x_+$

$$P' = -\frac{m}{2\pi} \left[1 - \frac{\sqrt{(x_+ + x)(x_- + x)}}{q^2/m} \right],$$

$$P'' = -\frac{m}{2\pi} \frac{\sqrt{(x_+ - x)(-x_- + x)}}{q^2/m},$$

(VI) for $x_+ < x$

$$P' = -\frac{m}{2\pi} \left[1 - \frac{-\sqrt{(x_+ - x)(x_- - x)} + \sqrt{(x_+ + x)(x_- + x)}}{q^2/m} \right],$$

$$P'' = 0.$$

Appendix C : Equivalence of $\delta_{SC}(Q, \omega)$ and $\delta(Q, \omega)$

We prove the equivalence of $\delta_{SC}(Q, \omega)$ and $\delta(Q, \omega)$ in the t -matrix approximation after Engelbrecht and Randeria.²⁹ Hereafter we fix Q and omit it. (For simplicity we take $Q \geq 2k_F$ so that we do not have to consider the contribution from the two-hole antibound state in the following discussion.) We define the scattering phase shift in a finite system as

$$\frac{\delta_{SC}(\omega_i)}{\pi} = -\frac{\omega_i - \omega_i^{(0)}}{\omega_{i+1}^{(0)} - \omega_i^{(0)}}$$

where $\omega_i^{(0)}$ is the energy eigenvalue for non-interacting particles determined by $K^{-1}(\omega_i^{(0)}) = 0$ and ω_i is the energy eigenvalue for $\omega_i^{(0)} < \omega_i < \omega_{i+1}^{(0)}$ in the t -matrix approximation determined by $K^{-1}(\omega_i) = -U$. The phase angle of the t -matrix is defined by

$$T(\omega + i\eta) = |T(\omega + i\eta)| \exp[i\delta(\omega)].$$

The t -matrix for complex energy variable, z , in a finite system is obtained as

$$T(z) = W \prod_i \left(\frac{z - \omega_i^{(0)}}{z - \omega_i} \right)$$

with W being a real constant, because the zeros and poles of the t -matrix are given by $K^{-1}(\omega_i^{(0)}) = 0$ and $K^{-1}(\omega_i) = -U$, respectively. By using the definition of $\delta_{SC}(\omega_i)$, $T(z)$ is rewritten as

$$T(z) = W \exp \left(\sum_i \ln \left[1 - \frac{\delta_{SC}(\omega_i)}{\pi} \frac{\omega_{i+1}^{(0)} - \omega_i^{(0)}}{z - \omega_i} \right] \right).$$

Next we expand the logarithm and take the thermodynamic limit to obtain

$$T(z) = W \exp \left[- \int_{x_0}^{\infty} \frac{d\omega'}{\pi} \frac{\delta_{SC}(\omega')}{z - \omega'} \right]$$

where x_0 is the threshold energy for two-particle excitations. Finally we set $z \rightarrow \omega + i\eta$ to obtain

$$T(\omega + i\eta) = W \exp\left[-P \int_{x_0}^{\infty} \frac{d\omega'}{\pi} \frac{\delta_{SC}(\omega')}{\omega - \omega'}\right] \exp[i\delta_{SC}(\omega)]$$

so that we conclude $\delta_{SC}(\omega) = \delta(\omega)$.

Appendix D : Thermodynamic Potential in t -matrix Approximation

The thermodynamic potential, Ω , in the t -matrix approximation, which is the sum of the processes as shown in Fig. 21 with the bare Green's function, is given by³³

$$\Omega - \Omega_0 = T \sum_{\omega_l} \sum_{\mathbf{q}} \ln[1 + UK(q, \omega_l)]$$

where Ω_0 is the thermodynamic potential for free electrons. By introducing the phase angle,

$$\delta(q, \omega) = -\arg[1 + UK(q, \omega + i\eta)],$$

we obtain

$$\Omega - \Omega_0 = - \sum_{\mathbf{q}} \int_{-\infty}^{\infty} d\omega n(\omega) \frac{\delta(q, \omega)}{\pi}$$

with $n(\omega)$ being the bose distribution function.

Appendix E : Hubbard approximation

We formulate the Hubbard approximation,³⁴ which is usually introduced as a decoupling in the equation of motion for the Green's function, at $T = 0$ diagrammatically as the particle-particle ladder approximation in the coordinate space.⁴³ Let us introduce the Green's function on a site for an \uparrow -spin electron

$$G_{\uparrow}(\varepsilon) = \frac{1}{\varepsilon - \Sigma(\varepsilon)}$$

in terms of the self-energy on the site, $\Sigma(\varepsilon)$. For a single site the interaction channel is limited to only the particle-particle ladder process. In the Hubbard approximation the dynamics of particles is neglected at the single site level so that the resulting self-energy is expressed diagrammatically as shown in Fig. 29 and given by

$$\Sigma(\varepsilon) = \int \frac{d\omega}{2\pi i} \frac{U}{1 + UK(\omega)} G_{\uparrow}^0(\omega - \varepsilon)$$

where

$$K(\omega) = \int \frac{d\varepsilon'}{2\pi i} G_{\uparrow}^0(\varepsilon') G_{\uparrow}^0(\omega - \varepsilon').$$

Here the Green's function for free particles are given probabilistically as

$$G_{\uparrow}^0(\varepsilon) = \frac{1}{\varepsilon + i\eta}$$

and

$$G_{\downarrow}^0(\varepsilon) = \frac{1-n}{\varepsilon + i\eta} + \frac{n}{\varepsilon - i\eta}$$

with n being the number of the \downarrow -spin electron per site. Thus

$$K(\omega) = -\frac{1-n}{\omega + i\eta}$$

so that

$$\Sigma(\varepsilon) = \frac{Un}{1 - U(1-n)/(\varepsilon + i\eta)}.$$

For the single site problem the Green's function is obtained as

$$G_{\uparrow}(\varepsilon) = \frac{1-n}{\omega + i\eta} + \frac{n}{\omega - U + i\eta}$$

as expected solely by the reason of probability. Finally the intersite hopping is taken into account and the resulting Green's function is given by

$$G_{\uparrow}(k, \varepsilon) = \frac{1}{G_{\uparrow}^{-1}(\varepsilon) - \xi_k}.$$

Appendix F : Beyond t -matrix Approximation

In this appendix we examine higher-order contributions in the low-density expansion beyond the t -matrix approximation. We examine the effective interaction vertex in the particle-hole channel or in the particle-particle channel.

F.1. Particle-Hole Channel

First we consider the interaction vertex in the particle-hole channel, which is a basic ingredient in the Fermi liquid theory, regarding the t -matrix as the irreducible vertex.

At low energy we can replace the t -matrix by the effective interaction constant, U^* , as introduced in Eq. (112). Thus here it is sufficient to consider the contribution of the diagram shown in Fig.30. The divergence of this vertex determined by

$$1 - U^*P(q=0, \omega=0) = 0,$$

corresponds to the ferromagnetic instability. But this condition is not satisfied if the low density expansion is well-defined when $U^*N(0) \ll 1$. Thus within this theory the ferromagnetic instability is absent.⁴⁴

F.2. Particle-Particle Channel

Next we consider the effective interaction vertex, Γ , constructed by the particle-particle (p-p) ladder processes with respect to the p-p irreducible vertex, Γ^0 , which contains no p-p pair propagators as shown in Fig.31

$$\Gamma = \frac{\Gamma^0}{1 + K\Gamma^0}.$$

If we take the bare interaction, U , as Γ^0 , the t -matrix approximation results. Next order terms in $1/\ln(k_c/k_F)$ of Γ^0 are given by the processes

as shown in Fig.32 containing one p-h pair propagator. The resulting effective interactions in the Cooper channel are given by

$$\Gamma_{kk'}^0 = U - U^2P(k+k', \omega=0) = U + U^2N(0)$$

for anti-parallel spins and

$$\Gamma_{kk'}^0 = U^2P(k-k', \omega=0) = -U^2N(0)$$

for parallel spins. The difference in the sign of the U^2 -terms comes from the fermion loop factor. Then $\Gamma_{kk'}^0$ is repulsive for anti-parallel spins and attractive for parallel spins. The superconducting instability of $\Gamma_{kk'}$ occurs in the triplet channel. But the instability is reached only after summing up infinite order terms in $1/\ln(k_c/k_F)$ and $\Gamma_{kk'}$ is a partial summation of a particular process, thus it can not be concluded whether the instability occurs.

Though our theory at low density does not require U to be small, it looks like the weak-coupling ferromagnetic spin fluctuation theory.⁴⁵ Our result is consistent with that obtained by Kotliar and Liu⁴⁶; they studied the superconducting instabilities in large U limit of a generalized Hubbard model with large spin degeneracy and found a p -wave instability at low density.

F.3. Landau Theory vs Kohn-Luttinger Mechanism

The Landau's Fermi-liquid theory³⁷ starts from a non-singular vertex of repulsive interaction without explicitly constructing the vertex on the Fermi surface which is an input parameter of the theory. Anderson¹² stressed that the breakdown of the Fermi-liquid theory originates from the construction of the vertex. For repulsive input parameters the renormalization group analysis in 2D^{38,39} assures that the Fermi-liquid fixed

point is stable. But unfortunately we have no reliable method to calculate the input parameters. If any of input parameters are attractive, the Fermi-liquid fixed point is excluded; one of such examples is the Kohn-Luttinger mechanism⁴⁷ of superconductivity where the input parameters are constructed perturbatively and another example is the spin fluctuation theory.⁴⁵ It should be noted that the input parameters are determined not only by low-energy processes but also by high-energy processes through renormalization transformations. In this context the plasmon mechanism of superconductivity^{48,49} for the electron gas has great importance.

References

1. J.G. Bednorz and K.A. Müller: *Z. Phys.* **B64** (1986) 189.
2. *Proceedings of the Anniversary Adriatico Research Conference and Workshop, Strongly Correlated Electron Systems*, Trieste, Italy, 1989 [*Int. J. Mod. Phys.* **B3** No.12 (1989)].
3. *Proceedings of the Anniversary Adriatico Research Conference and Miniworkshop, Strongly Correlated Electron Systems II*, Trieste, Italy, 1990 (World Scientific, 1991) eds. G. Baskaran, A.E. Ruckenstein, E. Tosatti and Yu Lu.
4. *Strong Correlation and Superconductivity* (Springer, 1989) eds. H. Fukuyama, S. Maekawa and A.P. Malozemoff.
5. *The Los Alamos Symposium 1989 High Temperature Superconductivity Proceedings* (Addison-Wesley, 1990) eds. K.S. Bedell, D. Coffey, D.E. Meltzer, D. Pines and J.R. Schrieffer.
6. J. Sólyom: *Adv. Phys.* **28** (1979) 201.
7. V.M. Galitskii: *Soviet Physics JETP* **34** (1958) 104.
8. P.W. Anderson: *Phys. Rev. Lett.* **64** (1990) 1839.
9. P.W. Anderson: *Phys. Rev. Lett.* **65** (1990) 2306.
10. P.W. Anderson: *Phys. Rev. Lett.* **66** (1991) 3226.
11. P.W. Anderson: *Phys. Rev. Lett.* **67** (1991) 2092.
12. P.W. Anderson: preprints.
13. W. Kohn and J.M. Luttinger: *Phys. Rev.* **118** (1960) 41.
14. F.D.M. Haldane: *J. Phys. C: Solid State Phys.* **14** (1981) 2585.
15. N. Kawakami and S-K. Yang: *J. Phys.: Condens. Matter* **3** (1991) 5983.
16. B. Doucot and X.G. Wen: *Phys. Rev.* **B40** (1989) 2719.
17. M. Ogata and H. Shiba: *Phys. Rev.* **B41** (1990) 2326.
18. T. Kopp, A.E. Ruckenstein and S. Schmitt-Rink: *Phys. Rev.* **B42** (1990) 6850.
19. *Fractional Statistics and Anyon Superconductivity* (World Scientific, 1990) F. Wilczek.

20. H. Fukuyama, Y. Hasegawa and O. Narikiyo: J. Phys. Soc. Jpn. **60** (1991) 2013.
21. F. Stern: Phys. Rev. Lett. **18** (1967) 546.
22. J. Lindhard: Kgl. Danske Videnskab, Selskab, Mat.-Fys. Medd. **28** (1954) No. 8.
23. C. Hodges, H. Smith and J.W. Wilkins: Phys. Rev. **B4** (1971) 302.
24. P. Bloom: Phys. Rev. **B12** (1975) 125.
25. S. Fujimoto: J. Phys. Soc. Jpn. **59** (1990) 2316.
26. J.R. Engelbrecht and M. Randeria: Phys. Rev. Lett. **65** (1990) 1032.
27. H. Fukuyama and Y. Hasegawa: Prog. Theor. Phys. Suppl. **101** (1990) 441.
28. M. Randeria: private communications.
29. J.R. Engelbrecht and M. Randeria: preprint.
30. J.R. Engelbrecht and M. Randeria: Phys. Rev. Lett. **66** (1991) 3225.
31. H. Fukuyama, O. Narikiyo and Y. Hasegawa: J. Phys. Soc. Jpn. **60** (1991) 372.
32. *Quantum Field Theoretical Methods in Statistical Physics* (Pergamon, 1965) A.A. Abrikosov, L.P. Gor'kov and I.Ye. Dzyaloshinskii.
33. P. Nozières and S. Schmitt-Rink: J. Low Temp. Phys. **59** (1985) 195.
34. J. Hubbard: Proc. Roy. Soc. **276** (1963) 237.
35. S. Fujimoto: Bussei Kenkyu **54** (1990) 207.
36. S. Schmitt-Rink, C.M. Varma and A.E. Ruckenstein: Phys. Rev. Lett. **63** (1989) 445.
37. L.D. Landau: Soviet Physics JETP **3** (1957) 920, **5** (1957) 101, **8** (1958) 70.
38. G. Benfatto and G. Gallavotti: Phys. Rev. **B42** (1990) 9967.
39. R. Shankar: Physica **A 177** (1991) 530.
40. C. Di Castro and W. Metzner: Phys. Rev. Lett. **67** (1991) 3852.
41. L.B. Ioffe and A.I. Larkin: Phys. Rev. **B39** (1989) 8988.

42. N. Nagaosa and P.A. Lee: Phys. Rev. Lett. **64** (1990) 2450.
43. S. Doniach: Adv. Phys. **18** (1969) 819.
44. J. Kanamori: Prog. Theor. Phys. **30** (1963) 275.
45. S. Nakajima: Prog. Theor. Phys. **50** (1973) 1101.
46. G. Kotliar and J. Liu: Phys. Rev. Lett. **61** (1988) 1784.
47. W. Kohn and J.M. Luttinger: Phys. Rev. Lett. **15** (1965) 524.
48. Y. Takada: J. Phys. Soc. Jpn. **45** (1978) 786.
49. Y. Takada: Phys. Rev. **B37** (1988) 155.

Figure Captions

- Fig. 1. Momentum distribution function of non-interacting fermions.
- Fig. 2. Momentum distribution function of Fermi liquids.
- Fig. 3. Momentum distribution function of Luttinger liquids.
- Fig. 4. Interaction Vertex.
- Fig. 5. Particle-particle correlation function $K(q, i\omega_l)$.
- Fig. 6. Characteristic energies for the particle-particle correlation function $K(q, x)$, x_0 and x_{\pm} , as a function of momentum q .
- Fig. 7. Real (a) and imaginary (b) parts of the particle-particle correlation function $K(q, x)$ as a function of momentum q and energy x .
- Fig. 8. Particle-particle correlation function $K(q, x)$ as a function of energy x for fixed momentum q . [$q = 0$ (a), k_F (b), $2k_F$ (c), $3k_F$ (d)] (The horizontal lines represent some typical interactions, $-U^{-1}$. The dotted horizontal lines in (a) and (c) represent the critical values, $-U_{c2}^{-1}$ and $-U_{c1}^{-1}$, respectively, for attractive interactions. The dot represents the two-particle/hole antibound state corresponding to the repulsive/attractive interaction. For attractive interactions the open circle represents the two-particle bound state.)
- Fig. 9. Contribution from $x \sim x_0$ to $K''(q, x)$ for $q < 2k_F$ (a) and $q > 2k_F$ (b).
- Fig. 10. Particle-hole correlation function $P(q, i\omega_l)$.
- Fig. 11. Characteristic energies for the particle-hole correlation function $P(q, x)$, $\pm x_{\pm}$, as a function of momentum q .
- Fig. 12. Real (a) and imaginary (b) parts of the particle-hole correlation function $P(q, x)$ as a function of momentum q and energy x .
- Fig. 13. Particle-hole correlation function $P(q, x)$ as a function of energy x for fixed momentum q . [$q = 0.2k_F$ (a), k_F (b), $2k_F$ (c), $3k_F$ (d)]
- Fig. 14. Diagrams resulting only in the shift in the chemical potential.
- Fig. 15. Self-energy corrections in second order of U in terms of the particle-particle correlation function (a) and the particle-hole correlation function (b).
- Fig. 16. Self-energy corrections in third order of U in the particle-particle channel (a) and the particle-hole channel (b).
- Fig. 17. Initial state (a) and intermediate scattering states in the second (b,c,d,e) and the third (f) order processes in U where the black and open dots represent electrons and holes, respectively, and the circle represents the Fermi surface.
- Fig. 18. Phase angle as a function of energy for $Q = 1.9k_F$ (a) and $Q = 2.1k_F$ (b).
- Fig. 19. Self-energy corrections, $\Sigma(k, i\varepsilon_n)$ (a), in terms of the t -matrix, $T(q, i\omega_l)$ (b).
- Fig. 20. Integration region for $\text{Im}\Sigma(k_F(\hat{\Omega}), \varepsilon + i\eta)$.
- Fig. 21. Generating functional for the self-consistent t -matrix approximation where the bold line represents \tilde{G} .
- Fig. 22. Self-energy in the self-consistent t -matrix approximation where the bold line represents \tilde{G} .
- Fig. 23. Self-energy expansion for the self-energy in the self-consistent t -matrix approximation.
- Fig. 24. Self-energy expansion for the self-energy in the self-consistent t -matrix approximation deduced from Fig.23(b).
- Fig. 25. Higher order self-energy expansion for the self-energy in the self-consistent t -matrix approximation.
- Fig. 26. Poles of the t -matrix in the case of negative U as a function of q for choices of $mU = -3.0$ (a), -5.0 (b) and -7.0 (c) with $k_c/k_F = 5.0$ so that $-mU_{c1} = -3.9$ and $-mU_{c2} = -6.7$.
- Fig. 27. Poles of the t -matrix as a function of negative U for $q = 0$ (a) and $q = 1.5k_F$ (b) with $k_c/k_F = 5.0$ so that $-mU_{c1} = -3.9$ and $-mU_{c2} = -6.7$.
- Fig. 28. Graphical solutions for the poles of the t -matrix given by $K = -U^{-1}$ where the vertical broken lines represent the poles for non-interacting particles given by $K^{-1} = 0$.
- Fig. 29. Self-energy process in Hubbard approximation.
- Fig. 30. Particle-hole ladder process based on the t -matrix.
- Fig. 31. Particle-particle ladder process.
- Fig. 32. Particle-particle irreducible vertex consisting of bubble or ladder process.

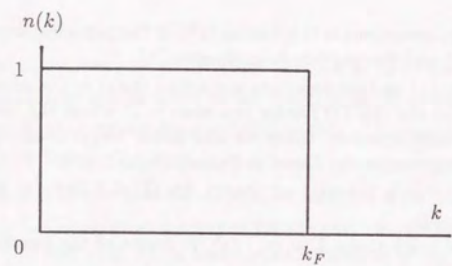


Fig. 1.

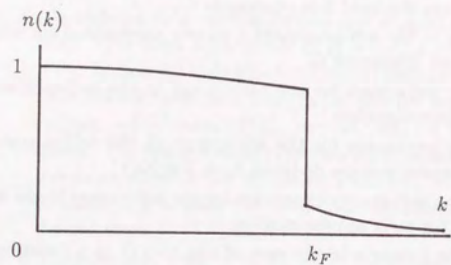


Fig. 2.

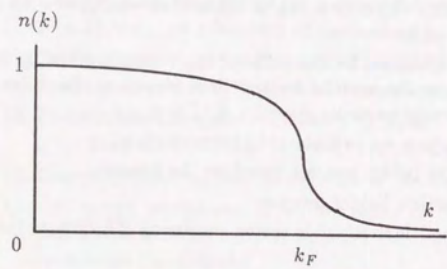


Fig. 3.

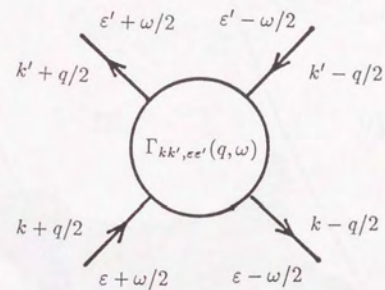


Fig. 4.

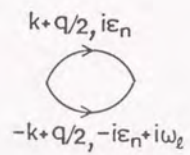


Fig. 5.

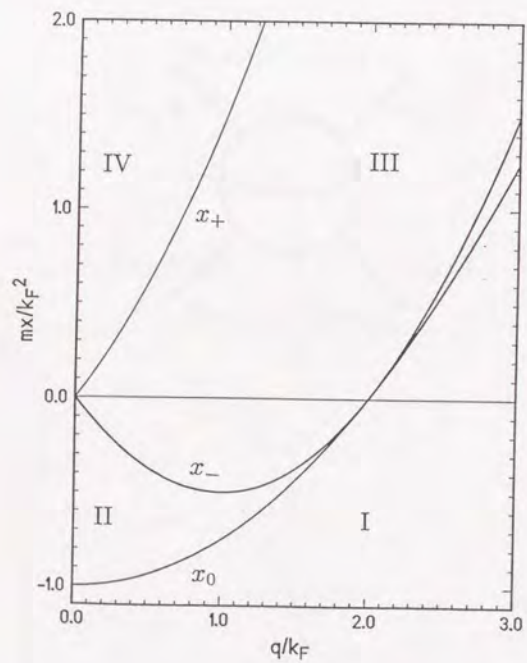


Fig. 6.

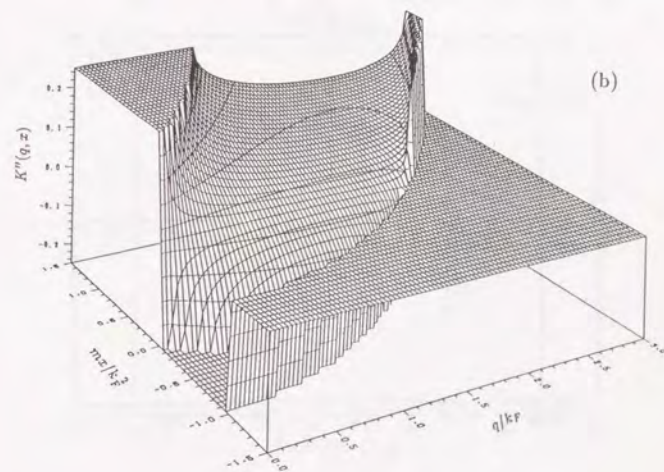
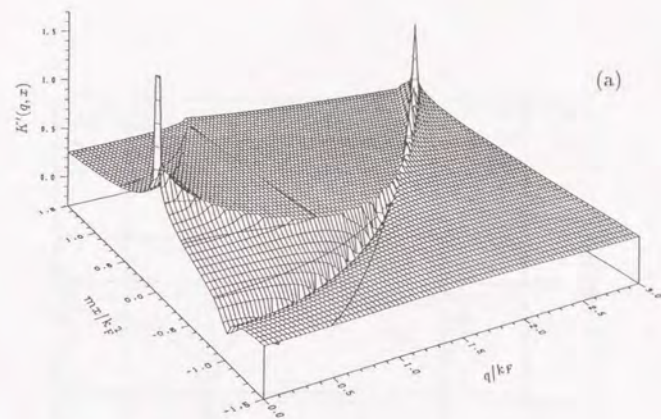


Fig. 7.

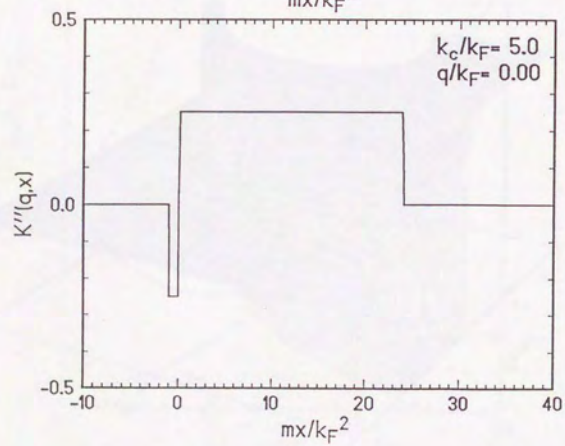
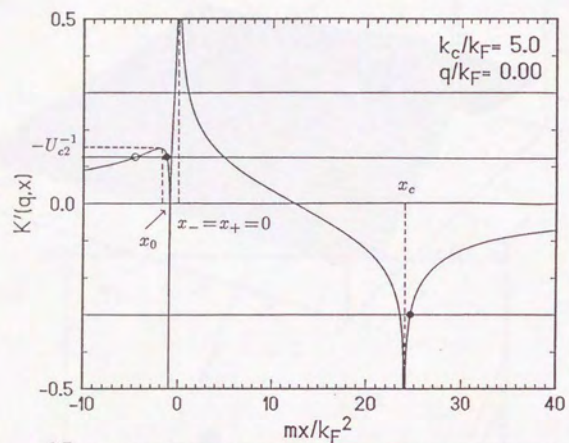
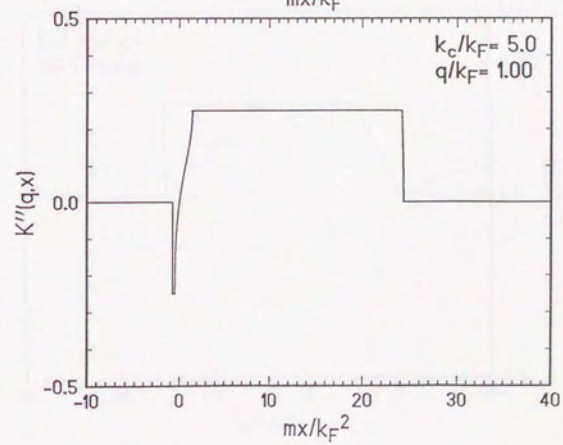
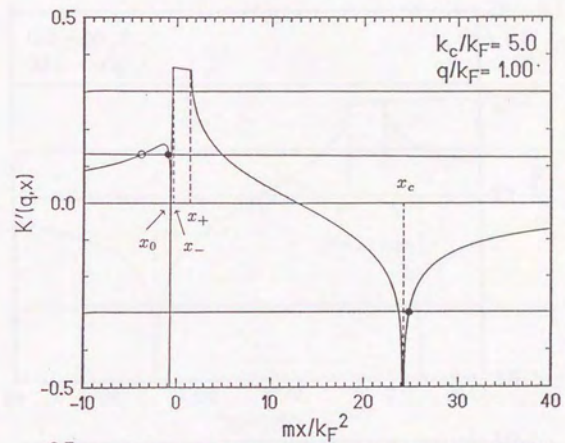
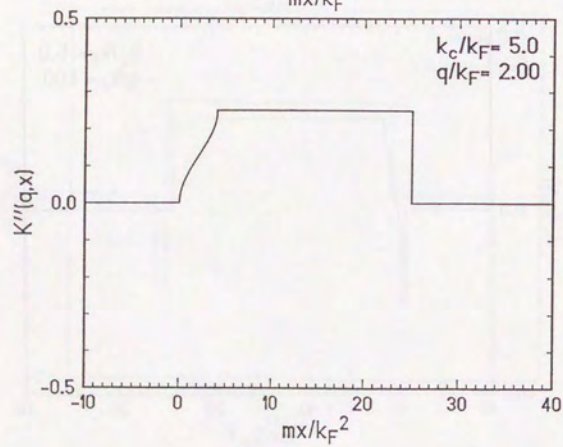
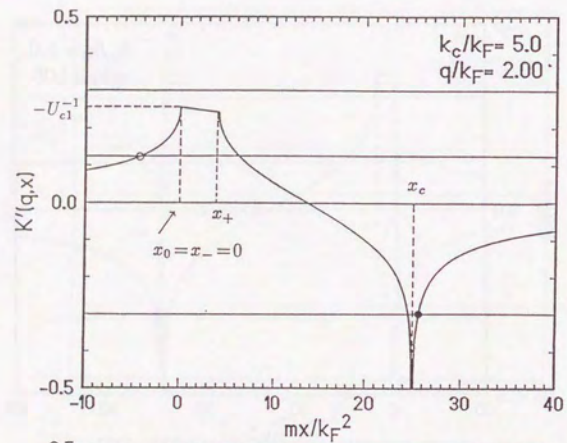


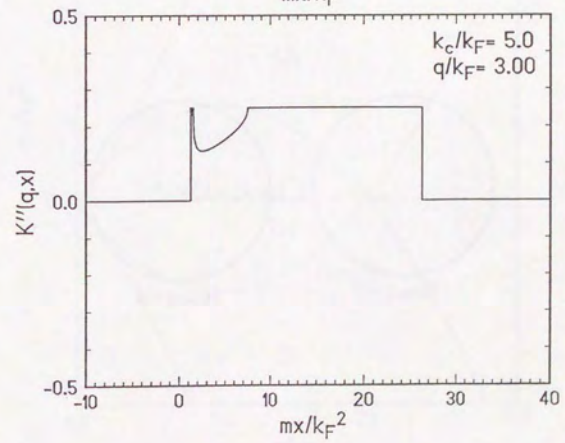
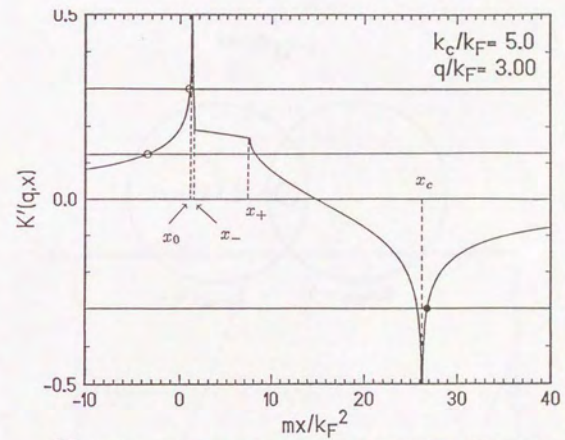
Fig. 8. (a)



(b)



(c)



(d)

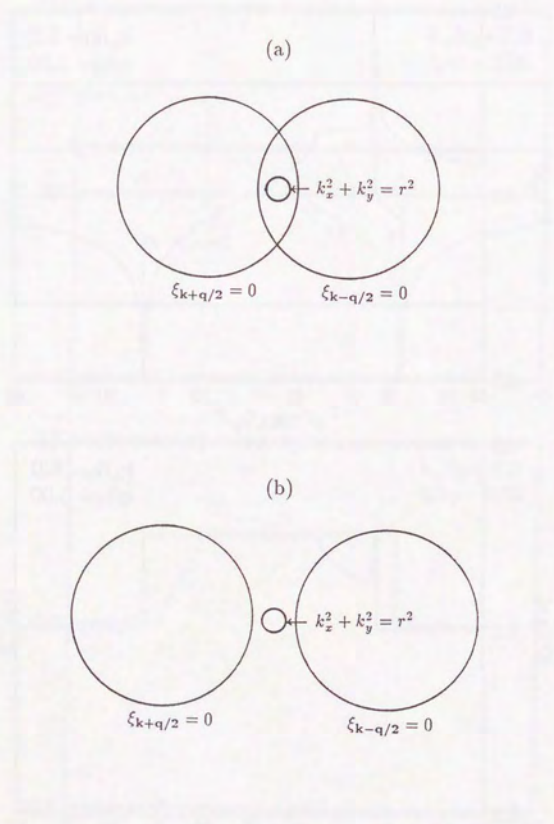


Fig. 9.

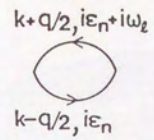


Fig. 10.

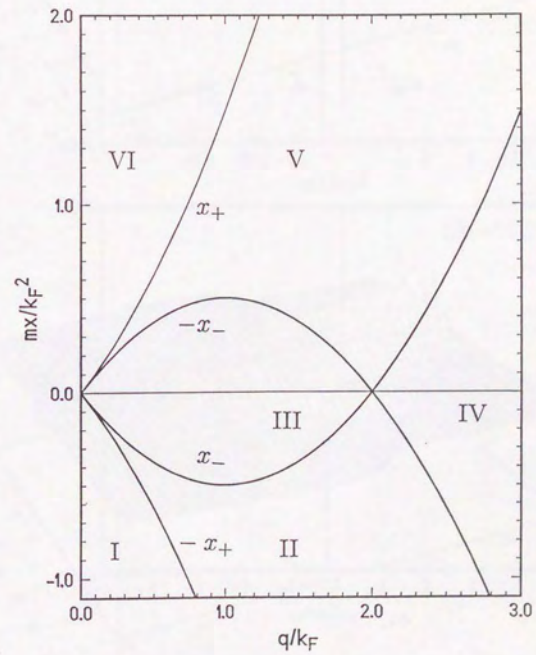


Fig. 11.

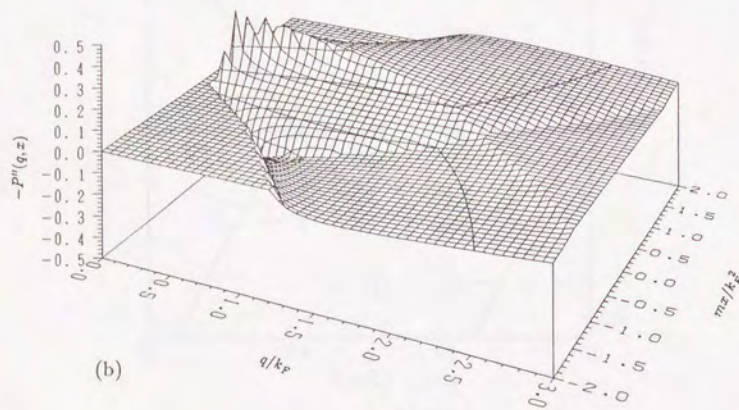
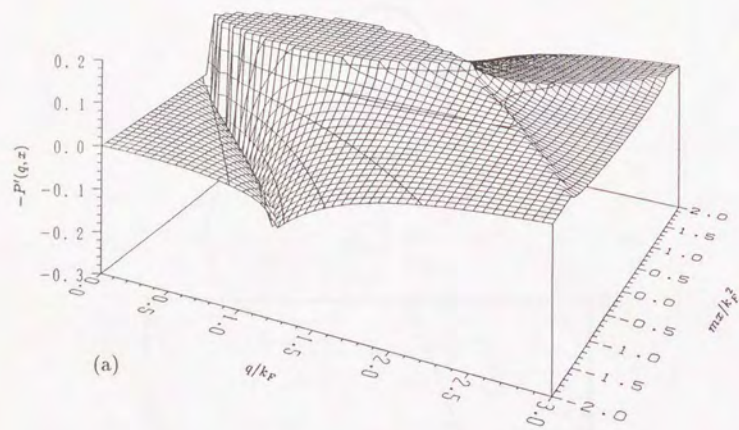


Fig. 12.

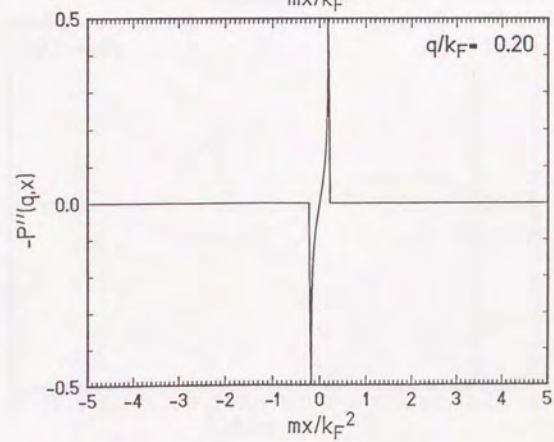
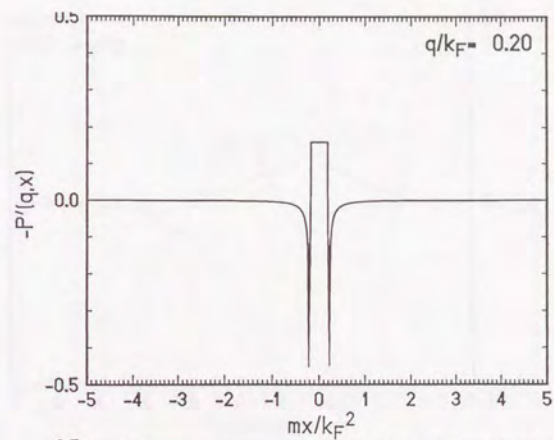
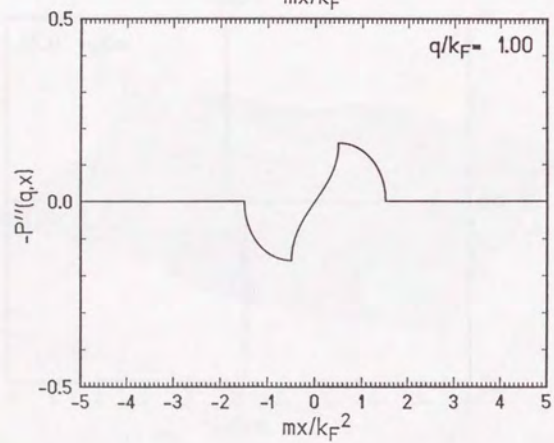
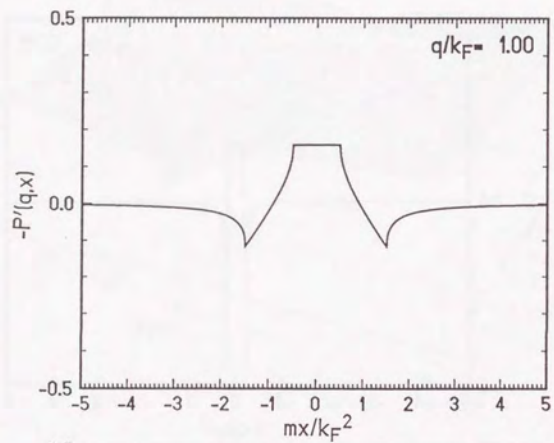
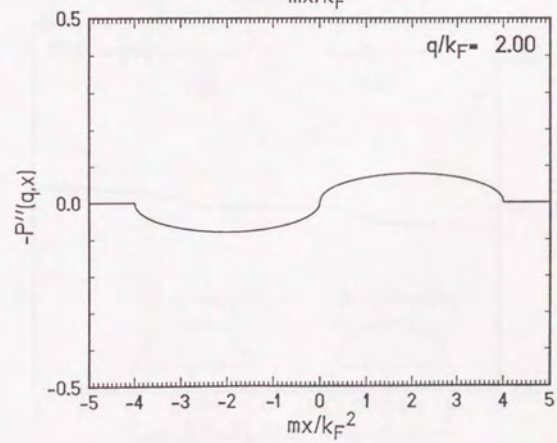
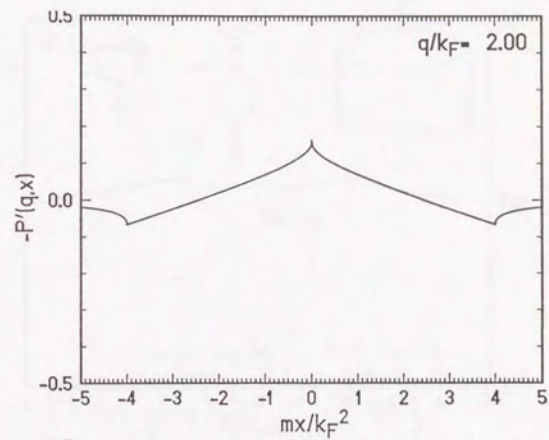


Fig. 13.

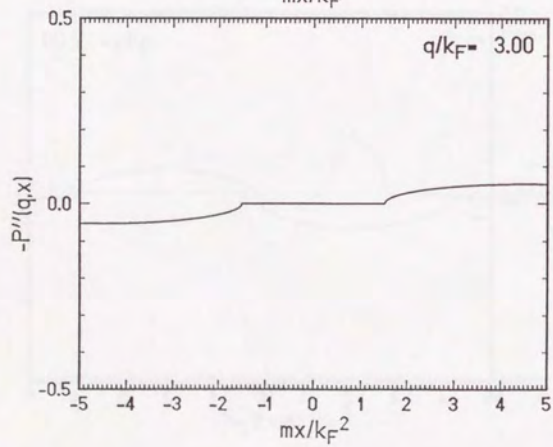
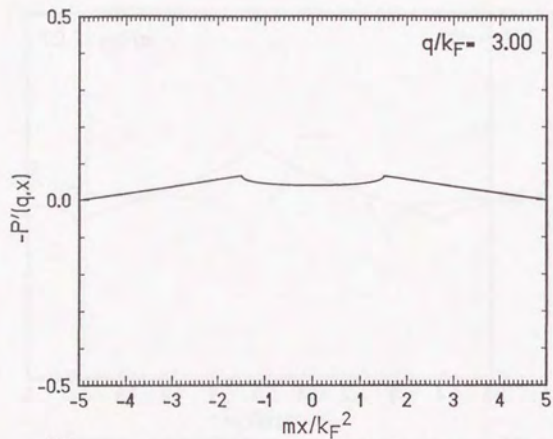
(a)



(b)



(c)



(d)

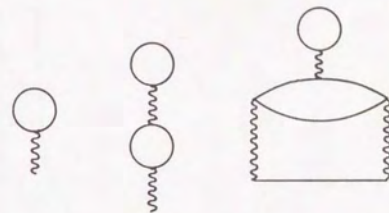


Fig. 14.

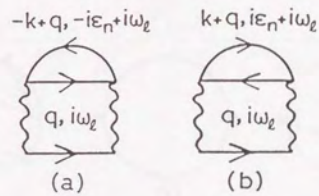


Fig. 15.

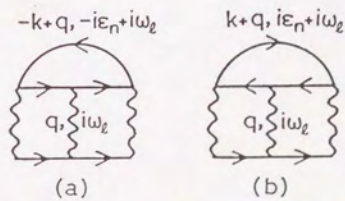


Fig. 16.

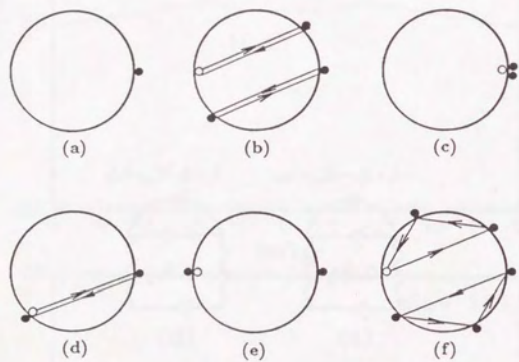
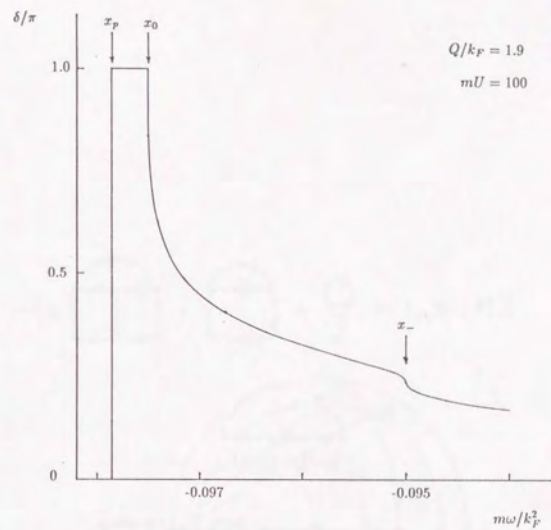
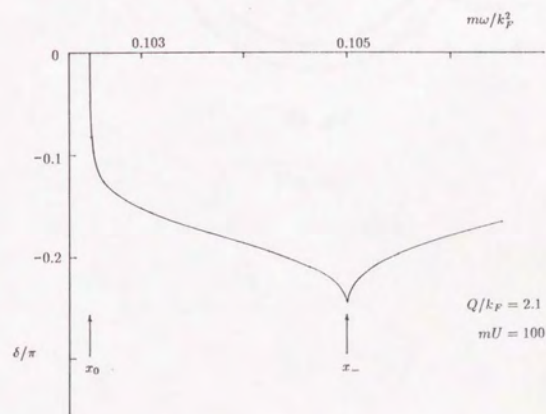


Fig. 17.

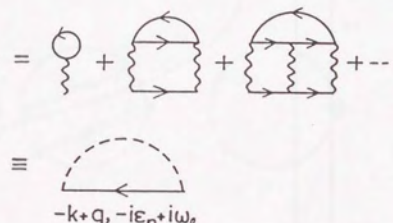


(a)



(b)

Fig. 18.

(a) $\Sigma(k, i\epsilon_n) =$ 

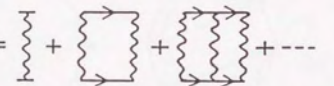
(b) $----- \equiv T(q, i\omega_2) =$ 

Fig. 19.

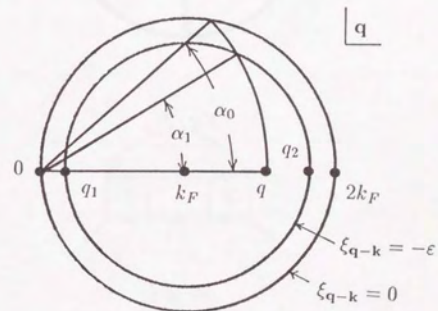


Fig. 20.

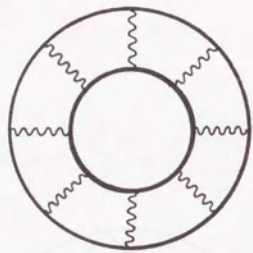


Fig. 21.

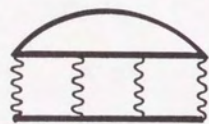


Fig. 22.

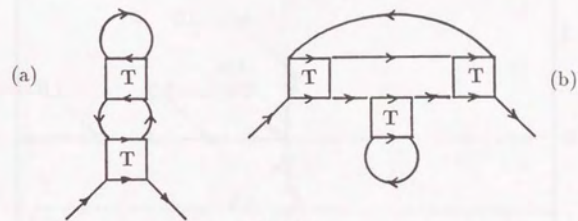


Fig. 23.

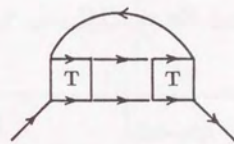


Fig. 24.

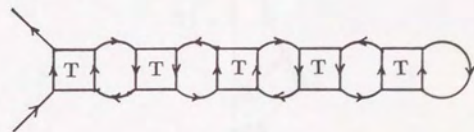


Fig. 25.

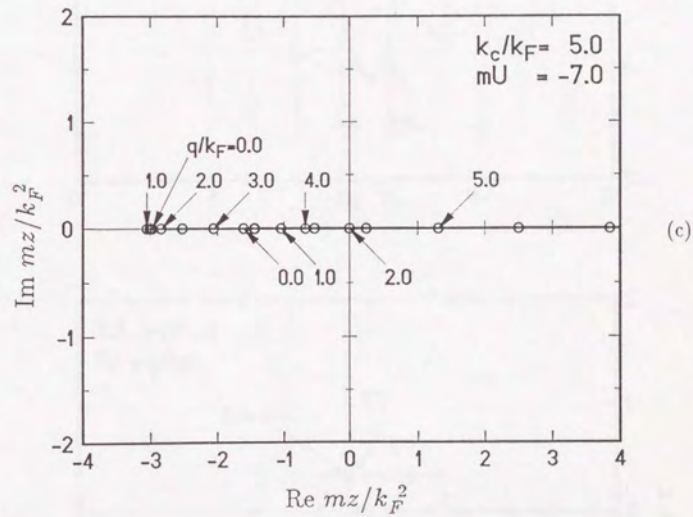
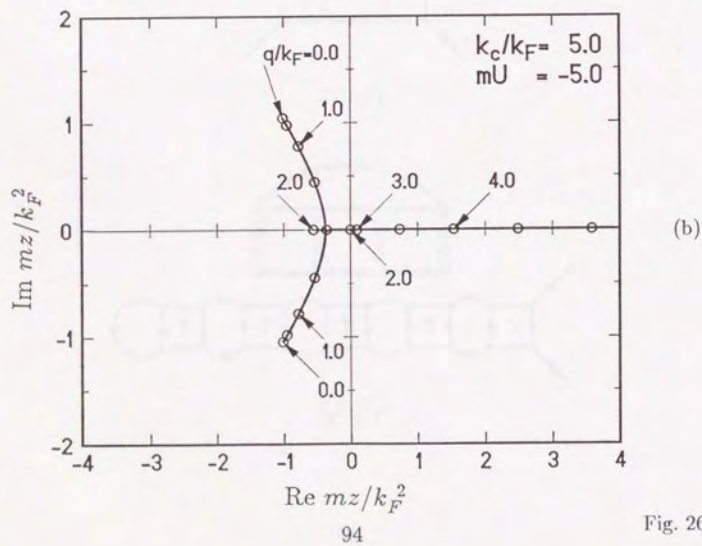
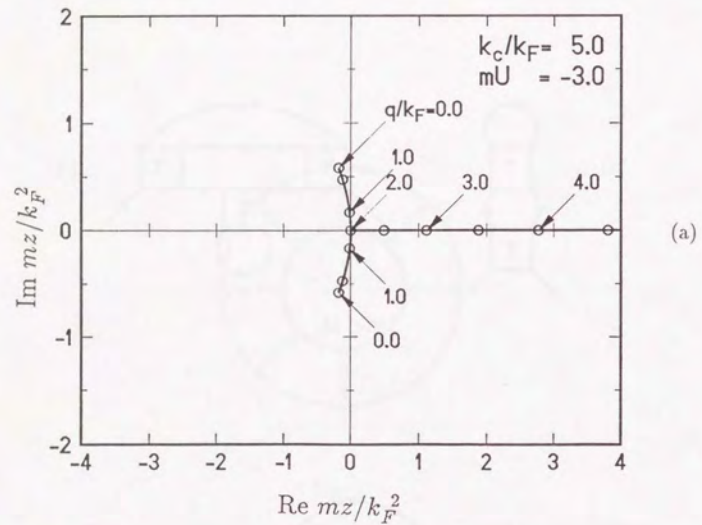
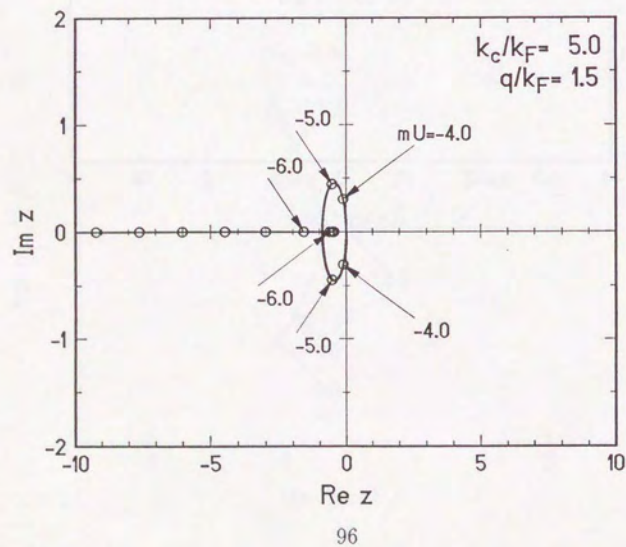
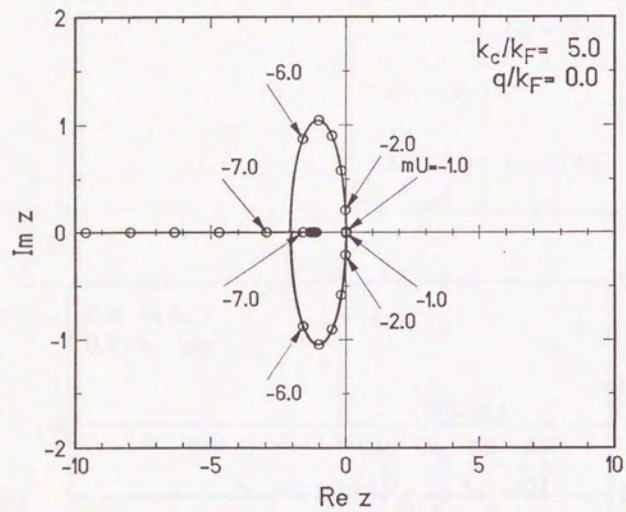


Fig. 26.



(a)

(b)

Fig. 27.

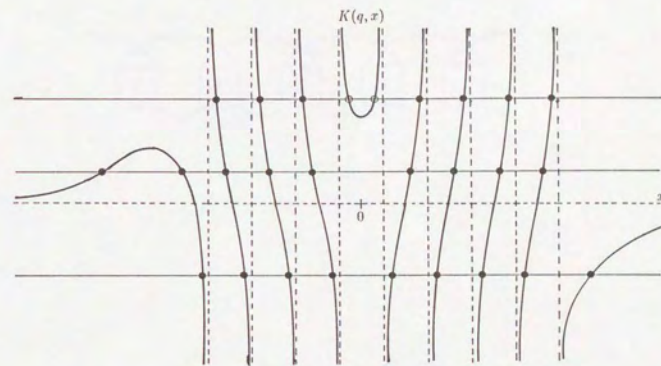


Fig. 28.

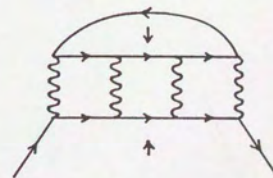


Fig. 29.

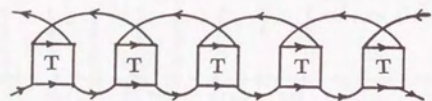


Fig. 30.

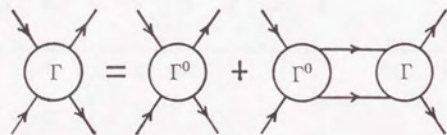


Fig. 31.

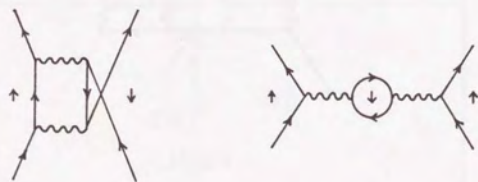


Fig. 32.

